Micro & nano-cooling: electronic cooling and thermometry based on superconducting tunnel junctions

Hervé Courtois

Néel Institute,
CNRS and Université Joseph Fourier, Grenoble, France

with L. Pascal, H. Nguyen, S. Rajauria, P. Gandit, T. Fournier, F. Hekking, B. Pannetier, C. Winkelmann

Summary

- Introduction
- The tunnel effect: a refresher
- Electron cooling and thermometry based on tunneling
- *Electron and phonon cooling in a S-I-N-I-S junction*
- Applications
- Conclusion

Introduction

Electronic cooling and thermometry

Electronic cooling from 300 mK down to 100 mK.

Electronic temperature directly measured.

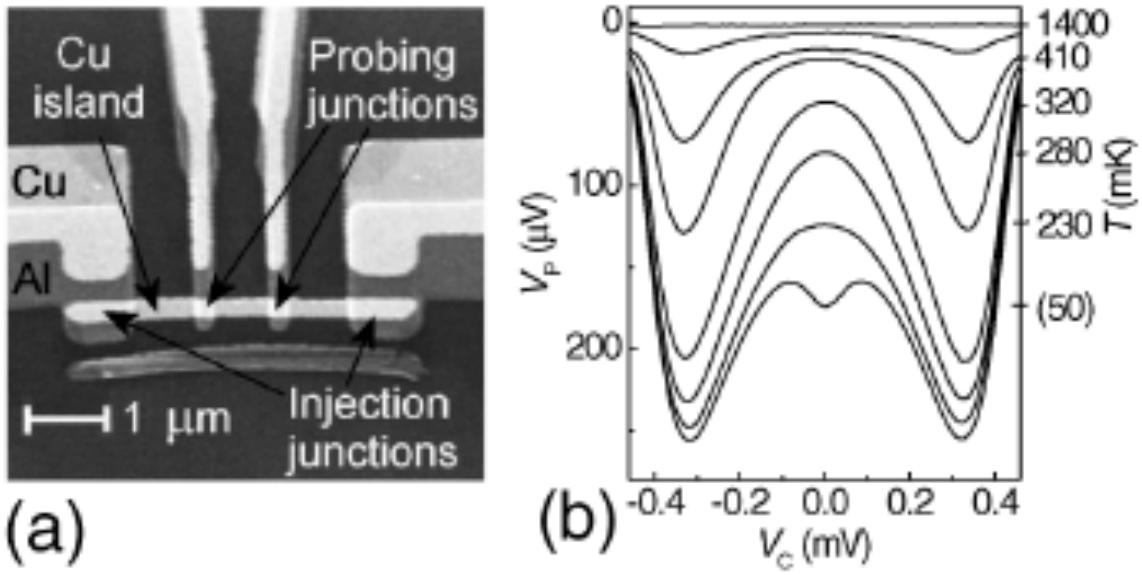

FIG. 1. Scanning electron micrograph of a typical cooler sample in (a), and cooling data in (b), where voltage V_P across the probe junctions in a constant current bias (28 pA) is shown against voltage V_C across the two injection junctions. Cryostat temperature, corresponding to the electron temperature on the N island at $V_C = 0$ is indicated on the right vertical axis. Below 100 mK this correspondence is uncertain, because of the lack of calibration and several competing effects to be discussed in the text.

J. Pekola, T.T. Heikkila, A. M. Savin, J.T. Flyktman, F. Giazotto, F.W.J. Hekking, Phys. Rev. Lett. 92, 056804 (2004): Helsinki.

Applications

Cooling of :
- sensors (bolometers)
- active devices (qbits, …)

Only the small electronic sensor is cooled.

A.M. Clark, N. A. Miller, A. Williams, S. T. Ruggiero, G. C. Hilton, L. R. Vale, J. A. Beall, K. D. Irwin, and J. N. Ullom, Appl. Phys. Lett. 84, 625 (2005): NIST Boulder.

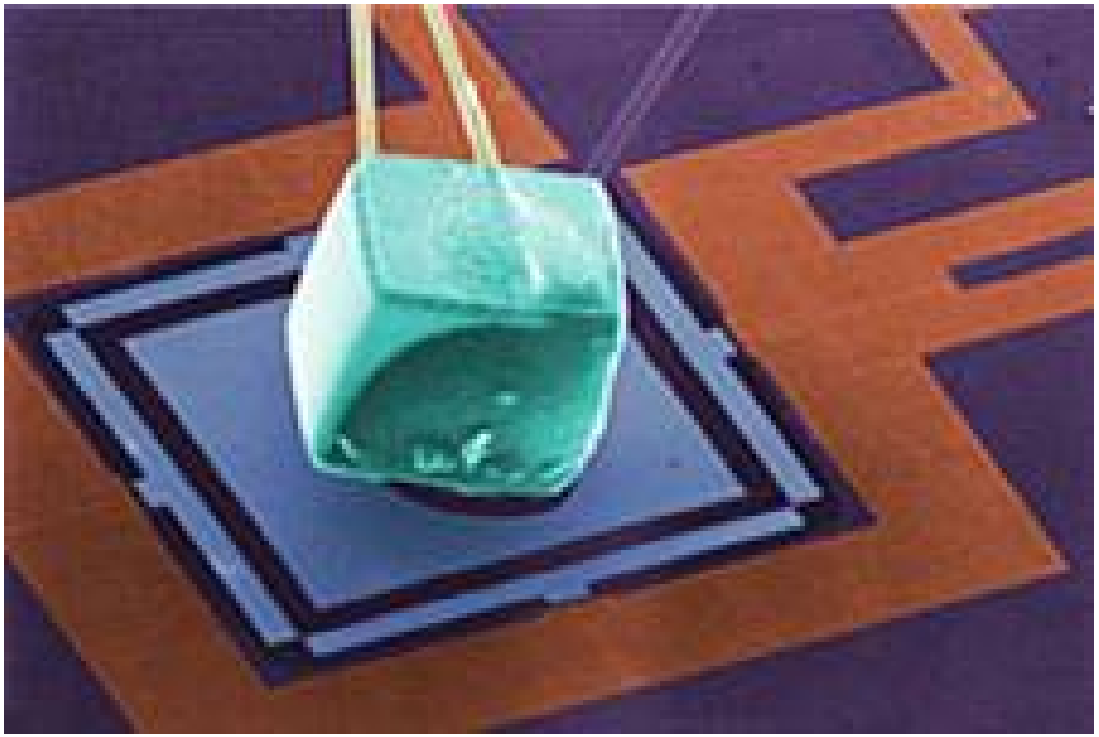

FIG. 2. Scanning electron microscope image of NIS refrigerator with attached neutron transmutation doped (NTD) germanium resistance thermometer. One of the four pairs of refrigerator junctions is circled. Additional junctions for thermometry are located beneath the NTD. The ratio of the volumes of the NTD and the refrigerating junctions is comparable to the ratio of the volumes of the Statue of Liberty and an ordinary person (about 11 000).

Pre-requisite

Electronic temperature

Non-zero temperature: the energy distribution function f(E) gives the probability for an e^- state at the energy E to be occupied.

At thermal equilibrium, f is the Fermi-Dirac function:

$$f(E) = \frac{1}{1 + \exp\left[\frac{E - E_F}{k_B T}\right]}$$

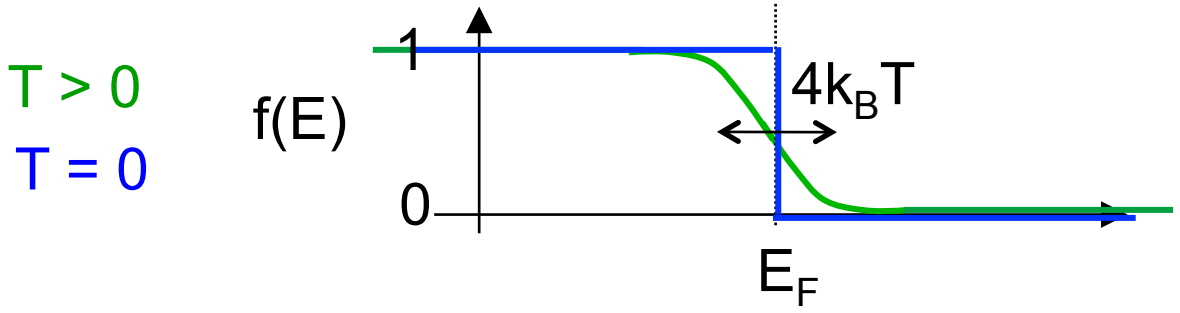

At zero temperature, it reduces to a step function.

Tunneling of electrons

Potential profile a the junction between two metals:

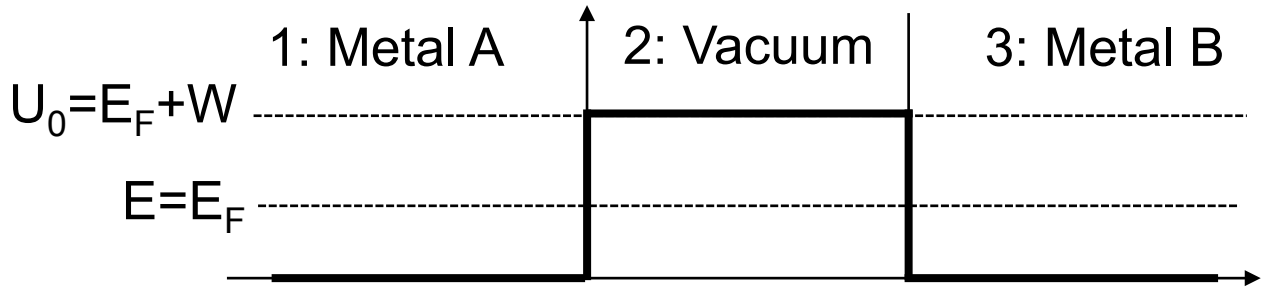

$$\Rightarrow \quad T \propto \exp\left(-2\alpha d\right) \qquad \alpha = \frac{\sqrt{2mW}}{\hbar}$$

Order of magnitude: $T = \exp\left(-10^{10} d\right)$

T is non negligible for d of the order of the Å.

A superconductor DOS spectra

Modified Density of States (DOS) at the Fermi Level

From BCS theory:

$$N_S(E) = 0 \quad \text{if} \left|E - E_F\right| < \Delta$$

$$N_S(E) = N_N \frac{\left|E\right|}{\sqrt{\left(E - E_F\right)^2 - \Delta^2}} \quad \text{if} \left|E - E_F\right| > \Delta$$

The energy gap is :

$\Delta(T=0) = 1.76 k_B T_c$

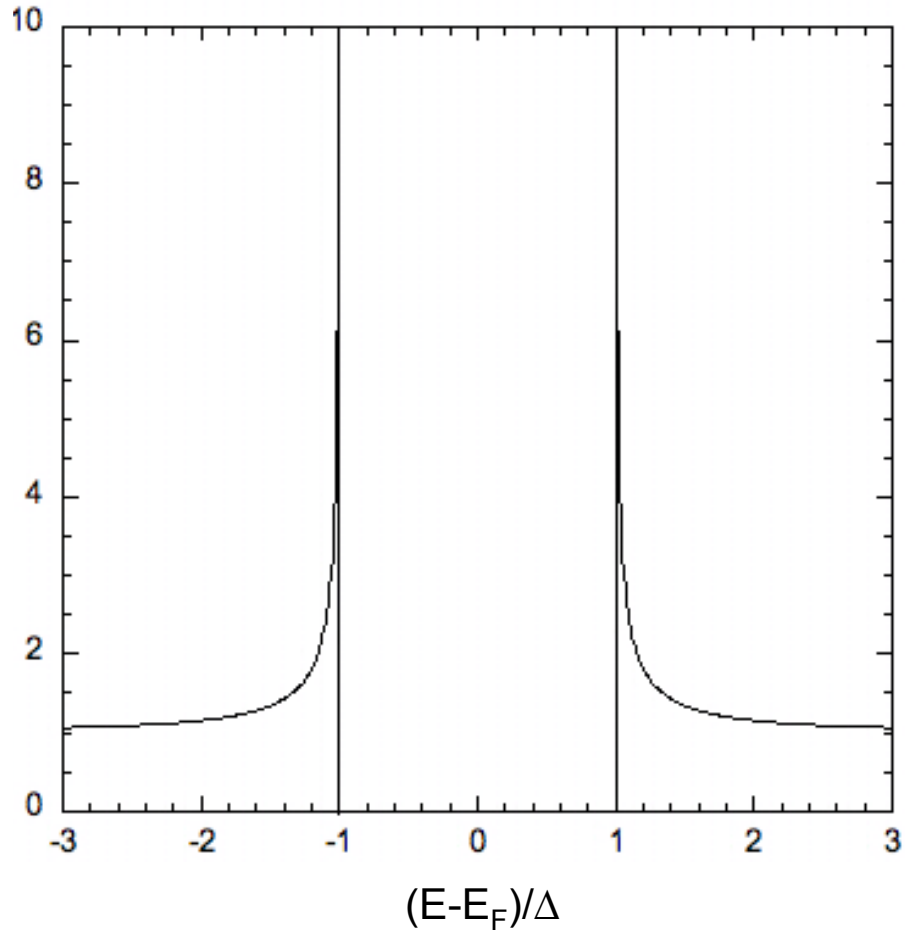

The tunnel current expression

Tunneling is an elastic process.

From Fermi golden rule:

$$I \propto \int_{-\infty}^{+\infty} N_A(E - eV) N_B(E) \left[f_A(E - eV) - f_B(E) \right] dE$$

A tunnel current occurs because of an electron states occupancy difference.

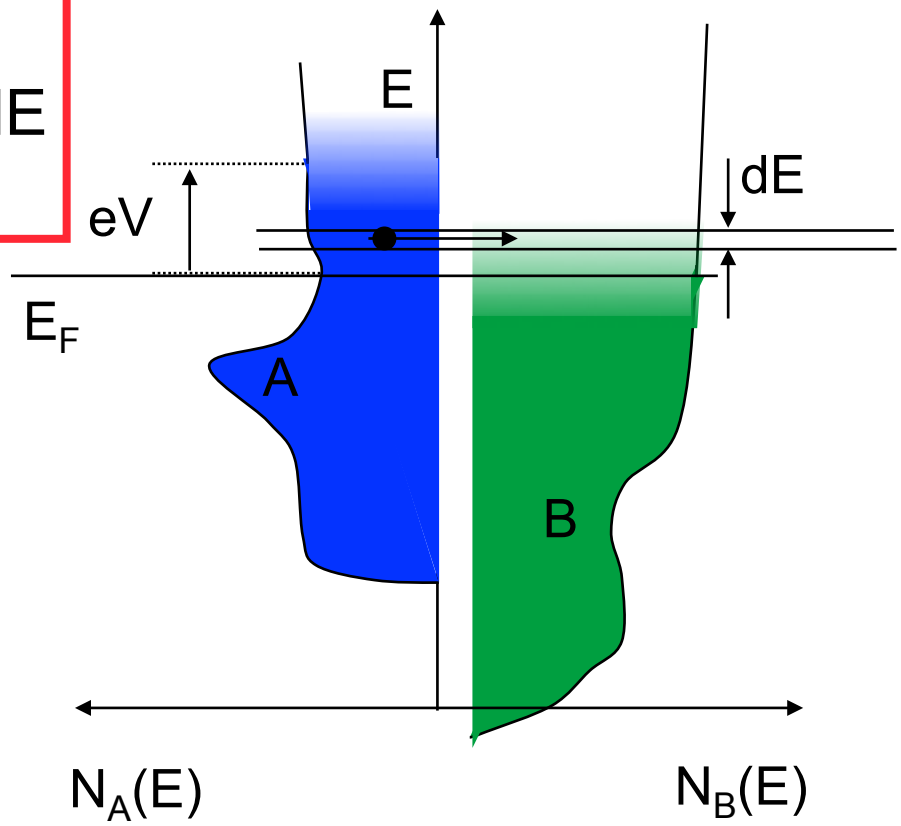

Electron thermometry in a S-I-N junction

Charge current in a N-I-S tunnel junction

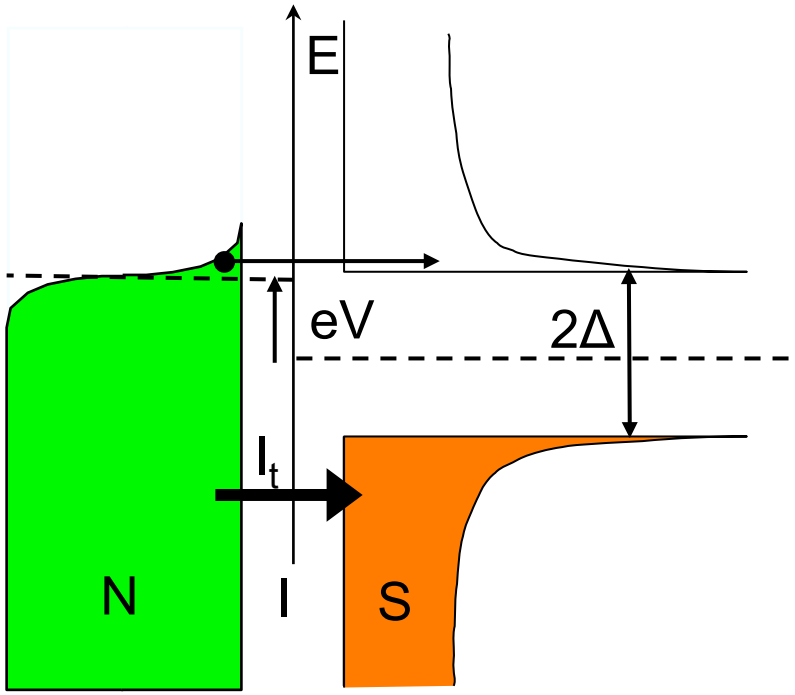

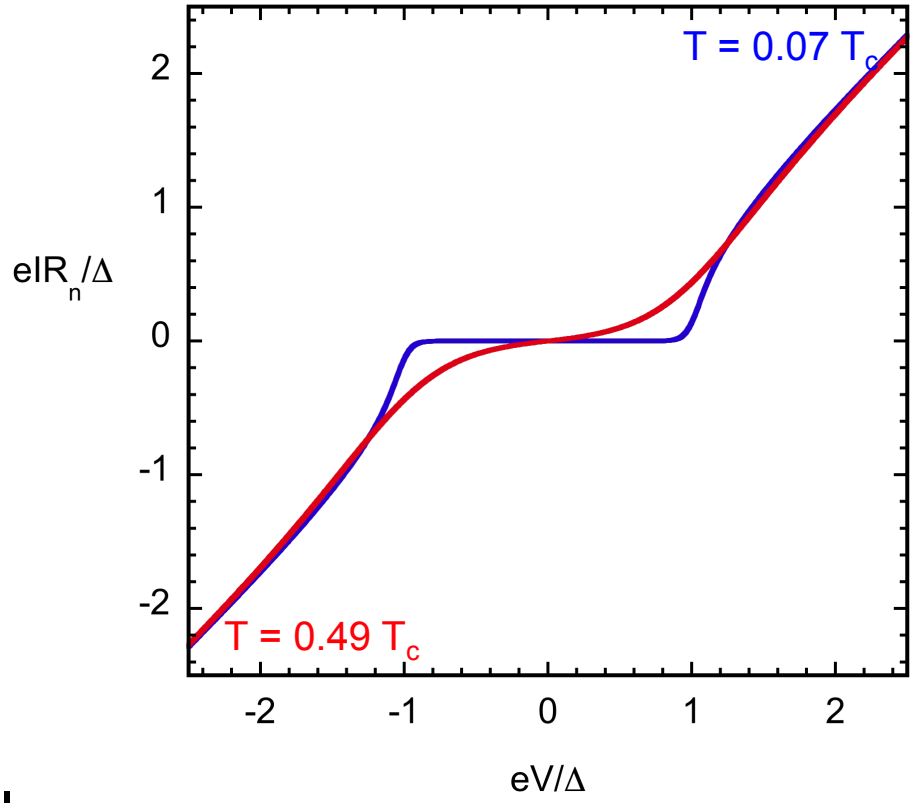

Only electrons above the gap can tunnel.

IV step rounded by temperature.

$$I_T = \frac{1}{eR_n}\int_{-\infty}^{+\infty} N_S(E)\left[f_S(E-eV) - f_N(E)\right]dE$$

Charge current in a N-I-S tunnel junction

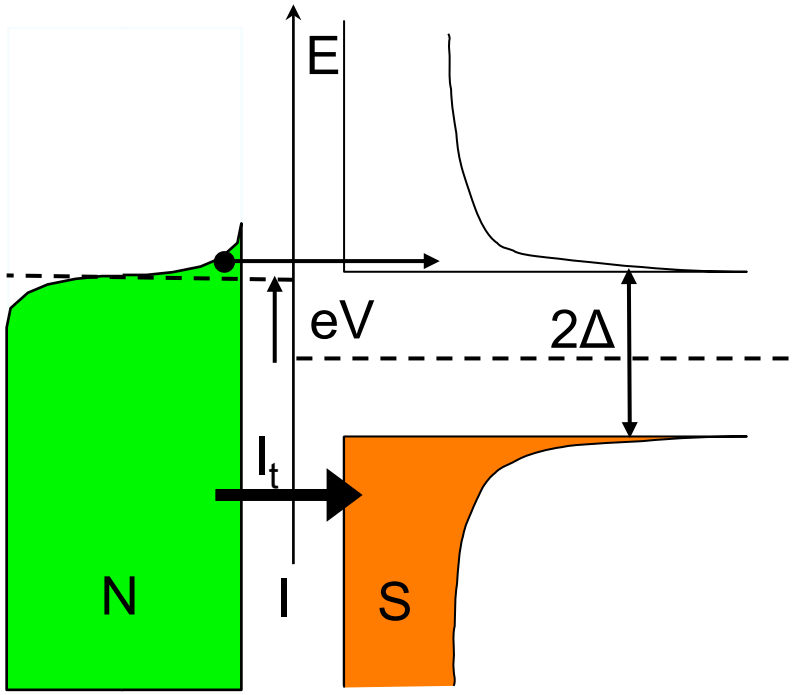

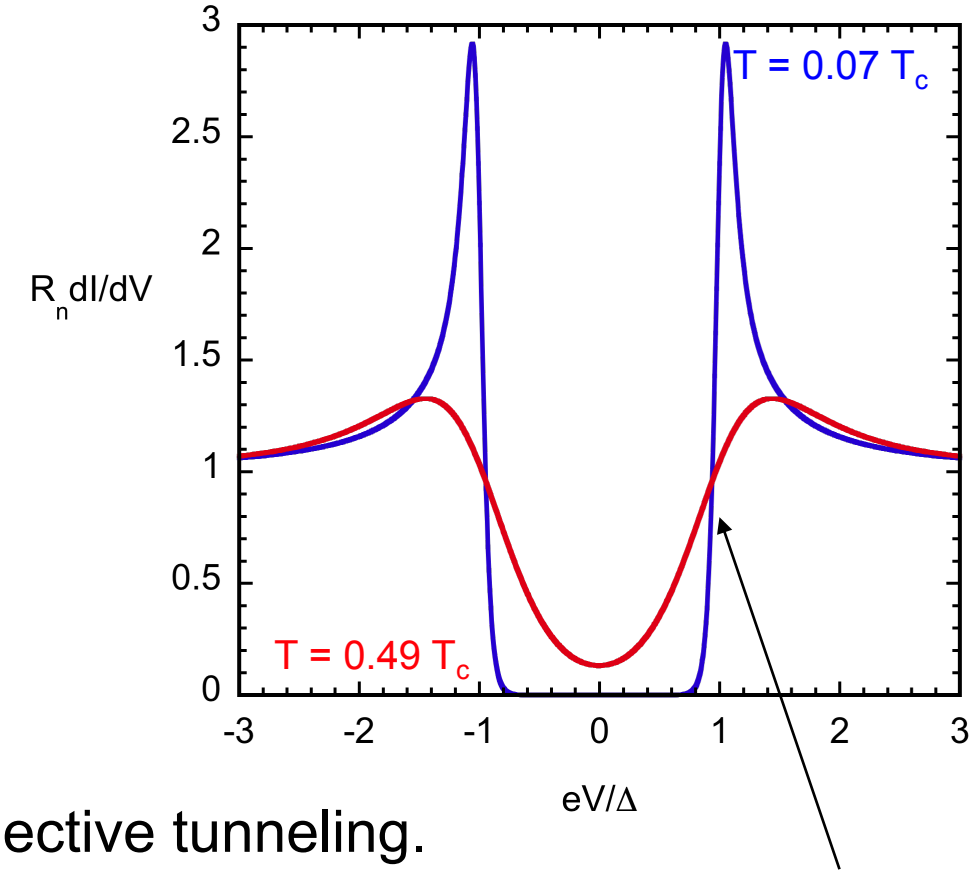

The energy gap induces an energy-selective tunneling.

Charge current (antisymmetric in bias):

$$I_T = \frac{1}{eR_n}\int_{-\infty}^{+\infty} N_S(E)\left[f_S(E-eV) - f_N(E)\right]dE$$

A N-I-S junction as a thermometer (1)

$$I = \frac{1}{eR_N}\int_{-\infty}^{+\infty} N_S(E)\left[f_N(E-eV) - f_S(E)\right]dE$$

DOS

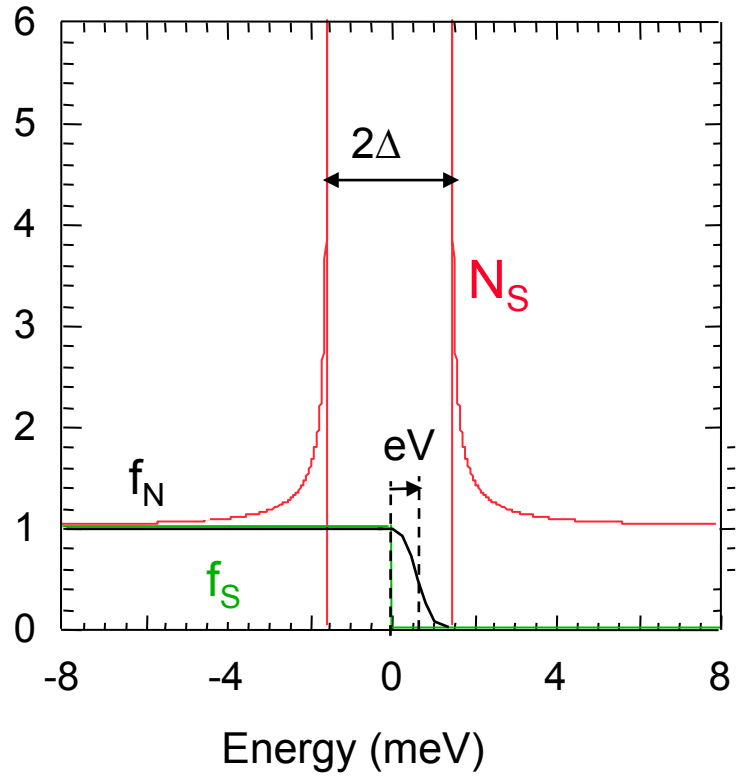

Consider T_S small, T_N to be measured,

$$eV < \Delta \approx E$$

$$f_N(E-eV) - f_S(E) \approx \exp\left(-\frac{E-eV}{k_B T}\right)$$

Sub-gap current:

$$eI = \frac{1}{R_N}\int_{-\infty}^{+\infty} N_S(E)\exp\left(-\frac{E-eV}{k_B T}\right)dE = eI_0\exp\left(\frac{eV}{k_B T}\right)$$

A N-I-S junction as a thermometer (2)

$$I = I_0 \exp\left(\frac{eV}{k_B T}\right)$$

The sub-gap current depends strongly on V and T.

$$\frac{dV}{dT} = \frac{k_B}{e} \ln\left(\frac{I}{I_0}\right) \approx 0.5\,\mu V/mK$$

M. Nahum and J. Martinis, Appl. Phys. Lett. 63, 3075 (1993).

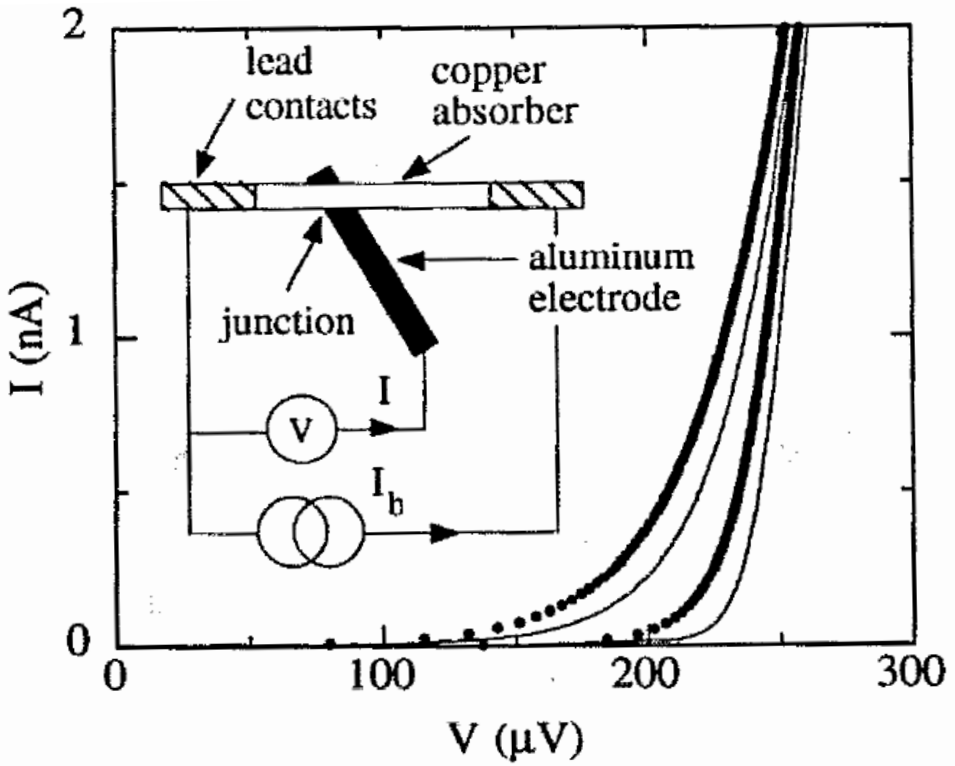

FIG. 1. Current-voltage characteristics of the SIN junction. The solid curves correspond to temperatures of 40 and 300 mK from right to left, with zero power dissipated in the absorber. The dotted curves correspond to a base temperature of 40 mK, but with 20 fW and 2 pW dissipated in the metal absorber, respectively. The inset is a schematic of the device. The power dissipated in the resistance R of the absorber is $I_b^2 R$.

Application of N-I-S junction thermometry

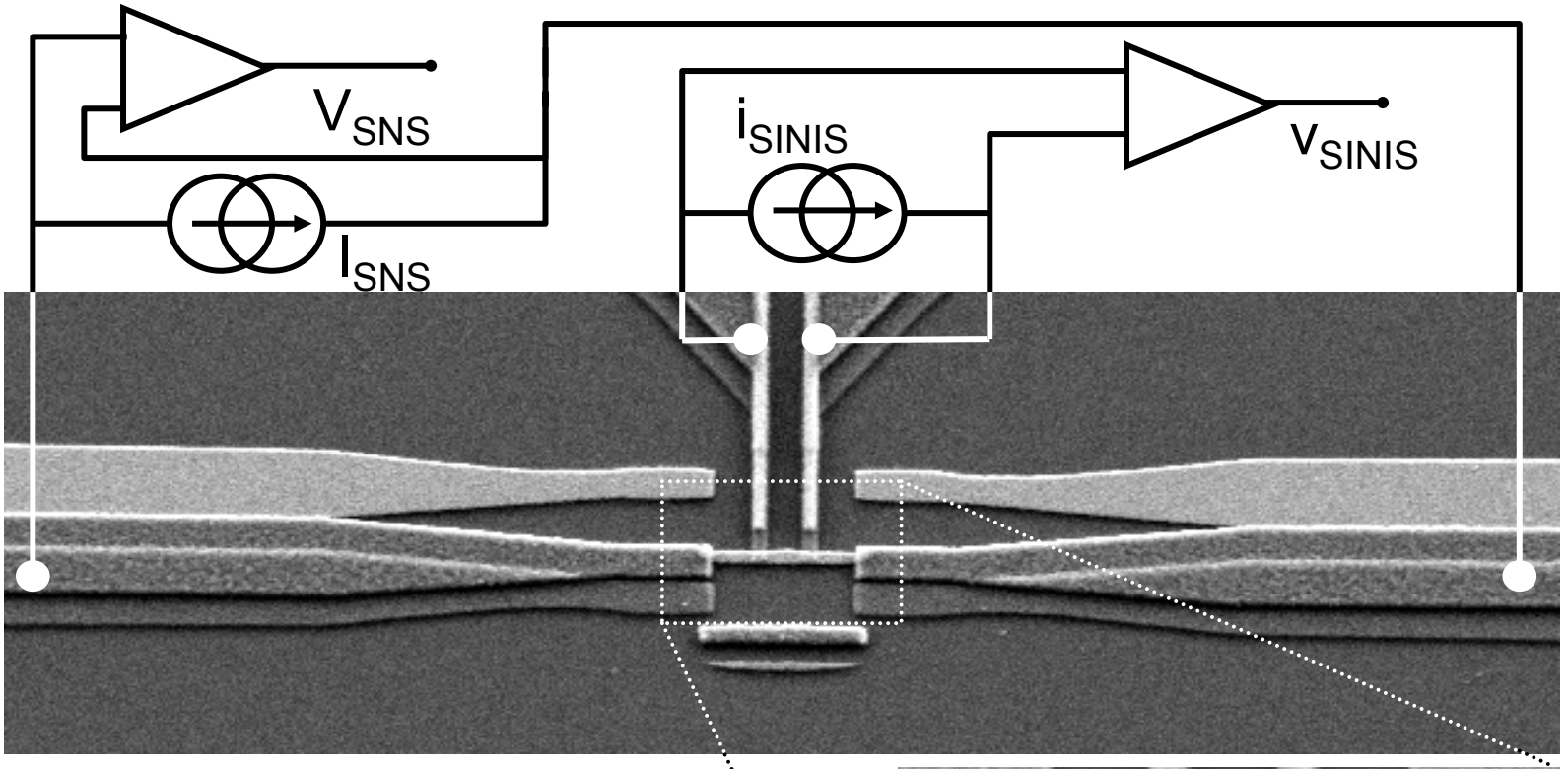

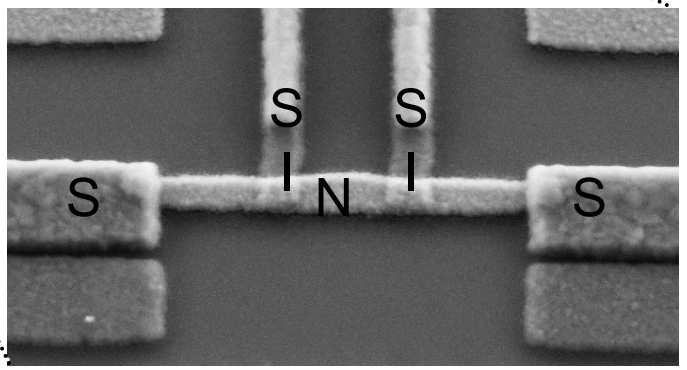

0.5 μm

L = 1.5 μm, w = 0.17 μm, t = 30 nm

R_N = 10 Ω : D = 100 cm^2/s, l_e = 22 nm

Thouless energy ε_c = 28 mK = 2.4 μeV

The SINIS thermometer calibration

I(V) of the double N-I-S junction at thermal equilibrium.

Calibration at a fixed current bias: no saturation down to 40 mK.

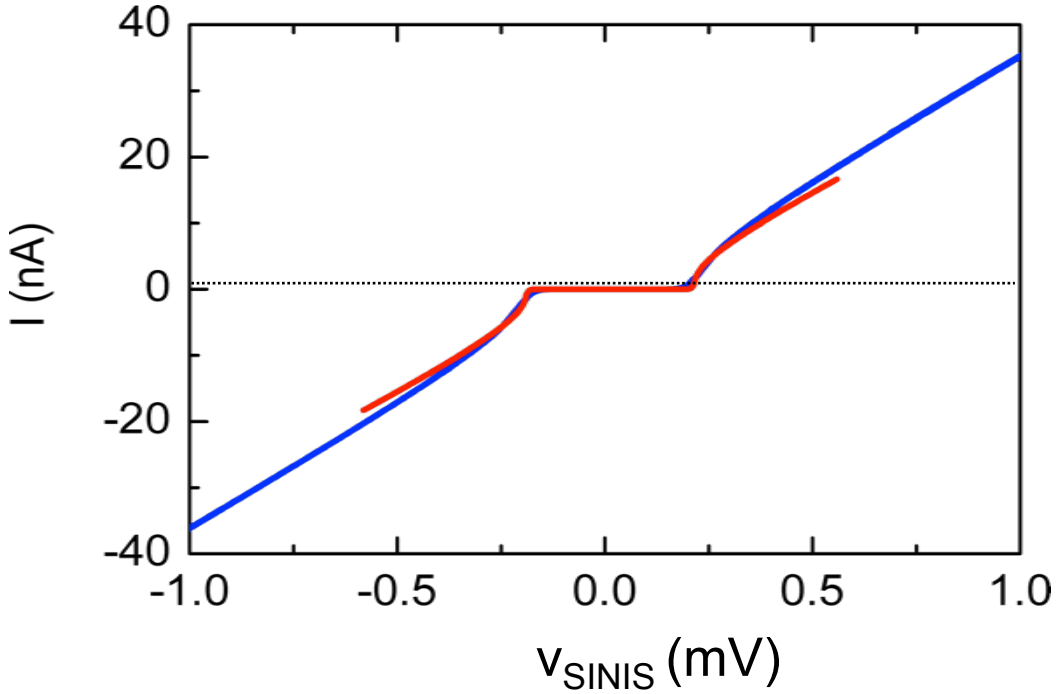

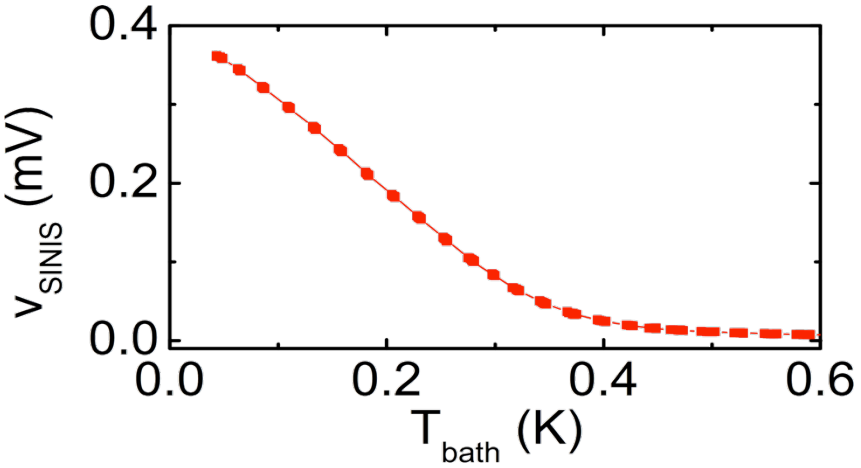

Hypothesis of quasi-equilibrium in the N metal: T_e can be defined.

I(V) and electron temperature

The electron thermometer correlates to switching.

thermal origin of the hysteresis. T_e up to 0.6 K !

H. Courtois, M. Meschke, J. T. Peltonen, and J. P. Pekola, PRL 101, 067002 (2008): Grenoble-Helsinki.

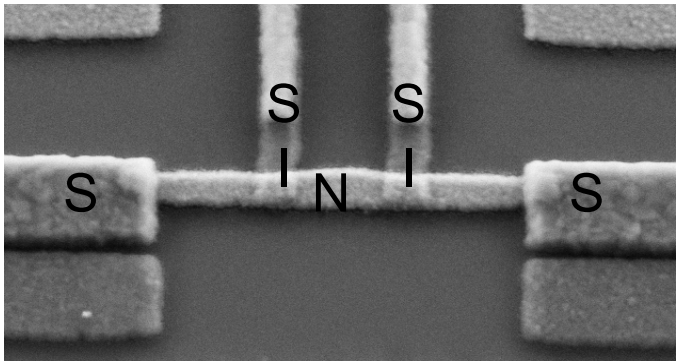

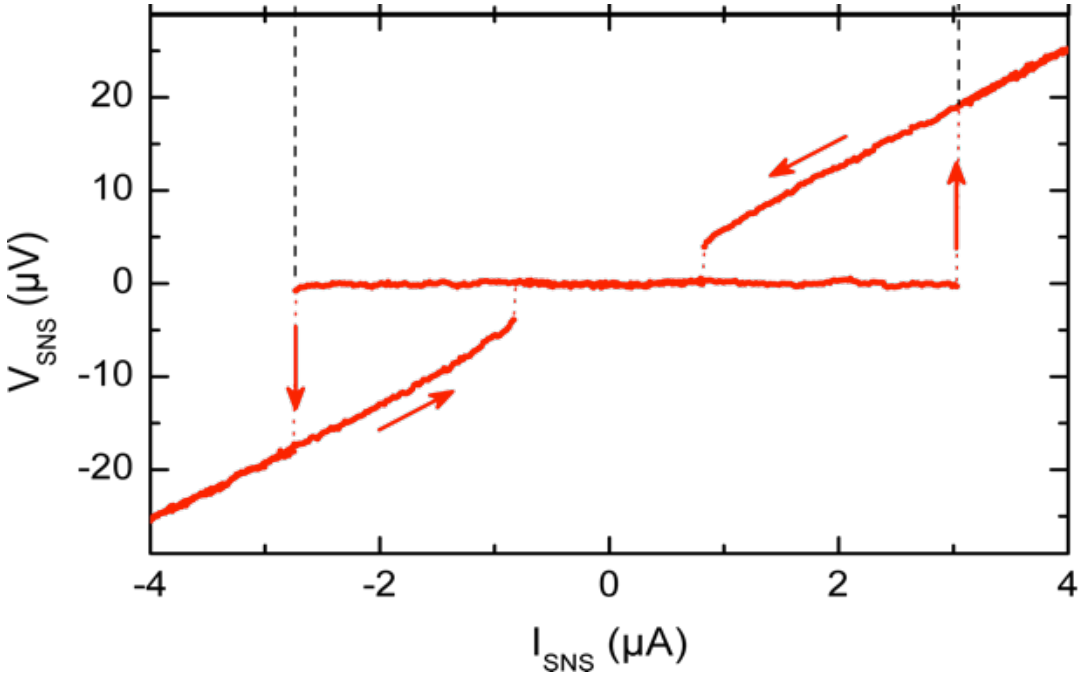

Electron cooling in a S-I-N-I-S junction

Charge current in a N-I-S tunnel junction

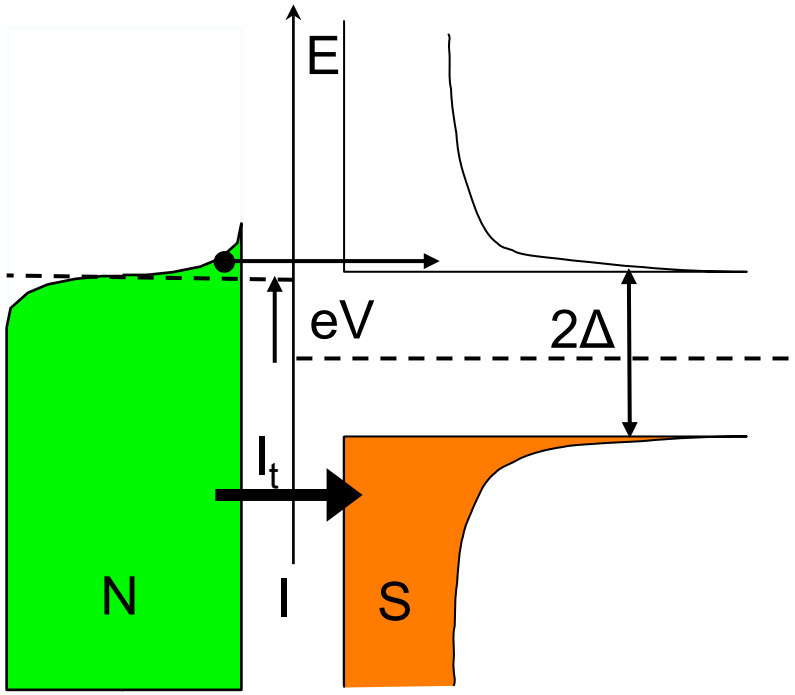

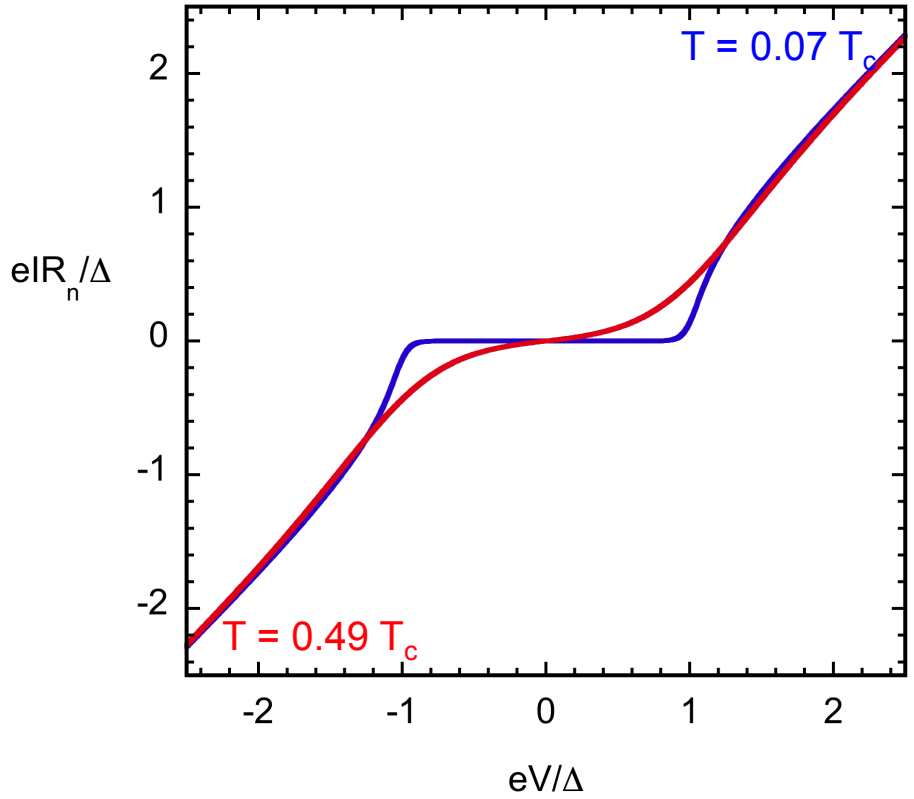

Only electrons above the gap can tunnel.

IV step rounded by temperature.

$$I_T = \frac{1}{eR_n}\int_{-\infty}^{+\infty} N_S(E)\left[f_S(E-eV) - f_N(E)\right]dE$$

Heat current in a N-I-S tunnel junction

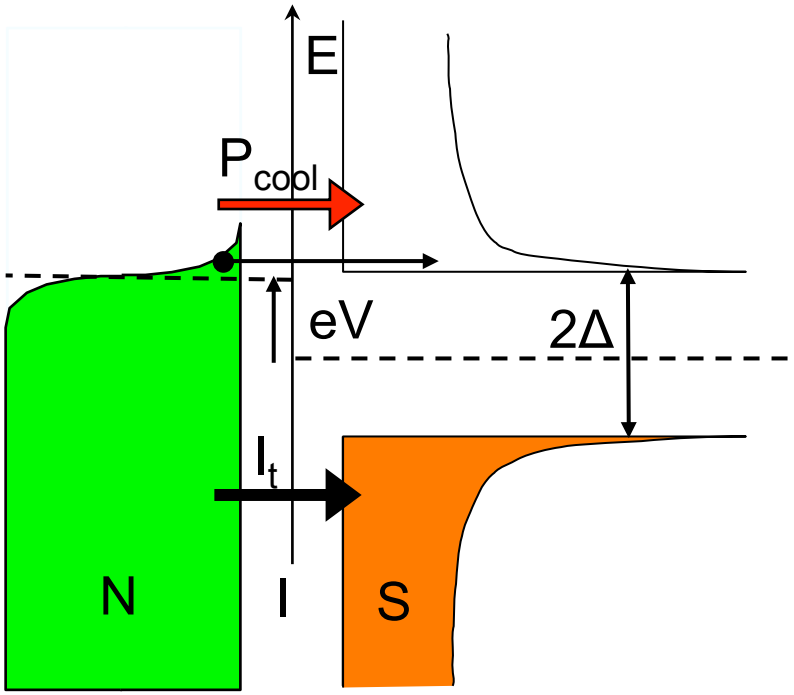

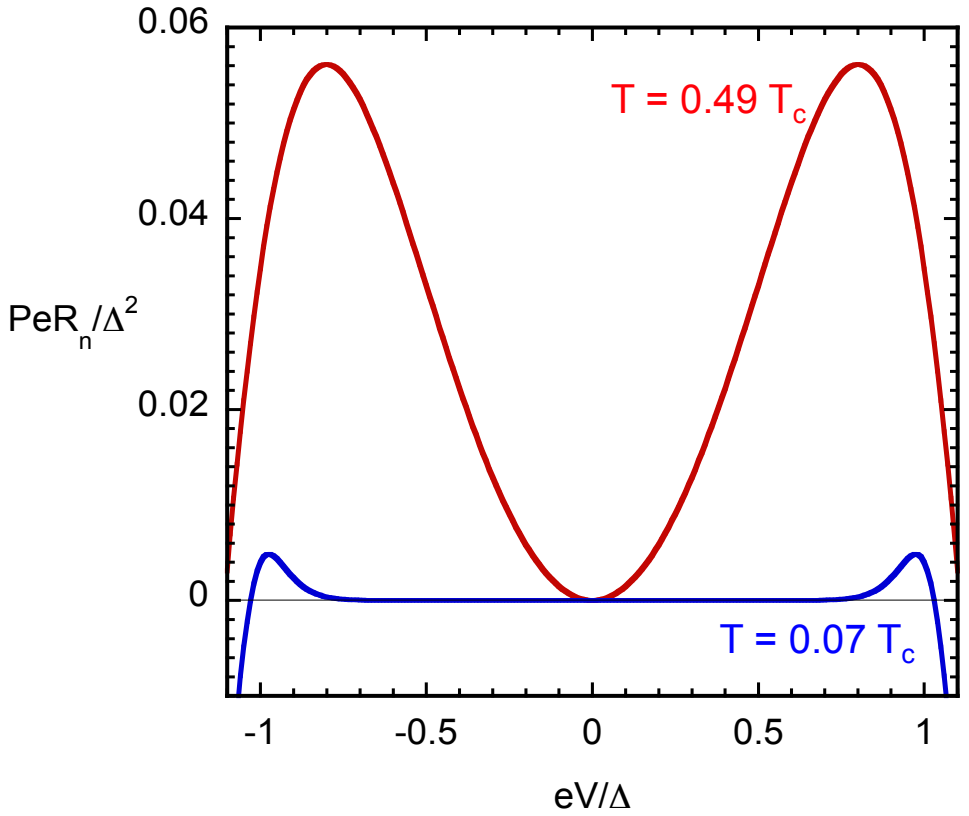

Heat current (symmetric in bias):

$$P_{cool}(V) = \frac{1}{e^2 R_n} \int_{-\infty}^{+\infty} (E - eV) N_S(E) \left[f_N(E - eV) - f_S(E) \right] dE$$

$I_T V + P_{cool}$ is deposited in S.

Cooling power

Bias-dependent, optimum

$$P_{max} = \frac{\Delta^2}{e^2 R_T}\left[0.59\left(\frac{k_B T_N}{\Delta}\right)^{3/2} - \sqrt{\frac{2\pi k_B T_S}{\Delta}}\exp\left(-\frac{\Delta}{k_B T_S}\right)\right]$$

$T_N << T_C$

reached at

$$V \approx \Delta/e - k_B T$$

Max cooling power at:

$$T \approx T_C/3$$

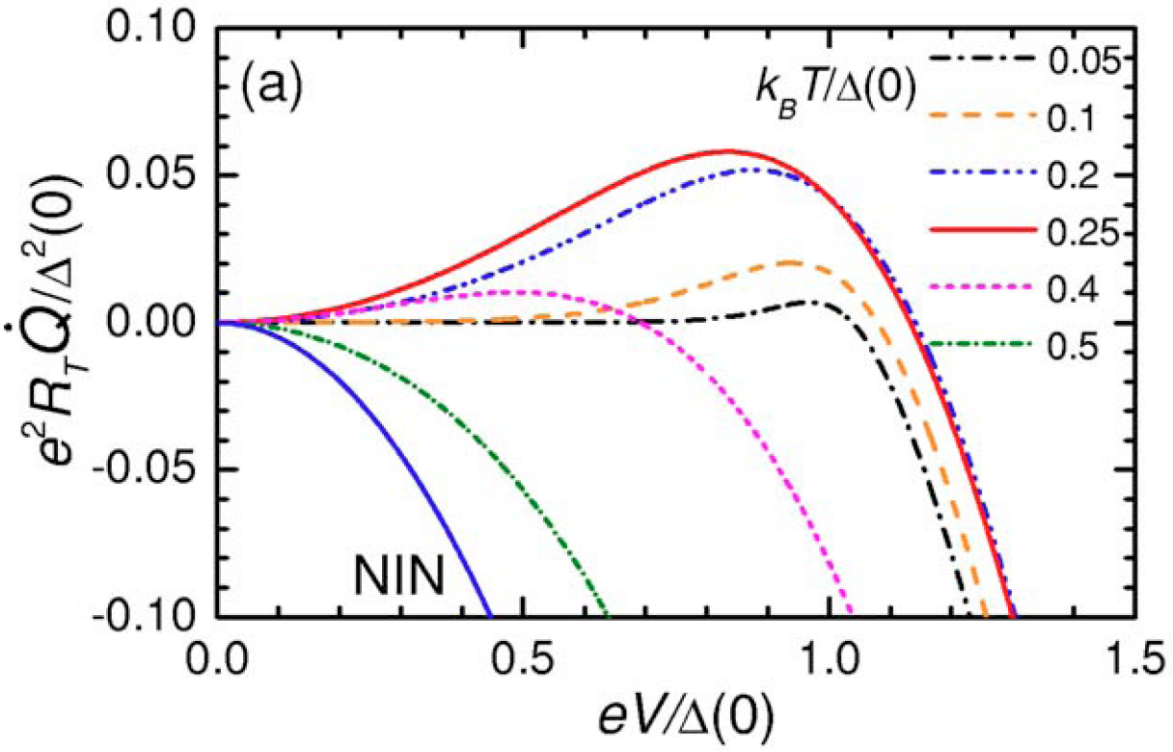

The S-I-N-I-S geometry

Two cooling junctions in series:
double cooling power + good thermal insulation of cooled metal.

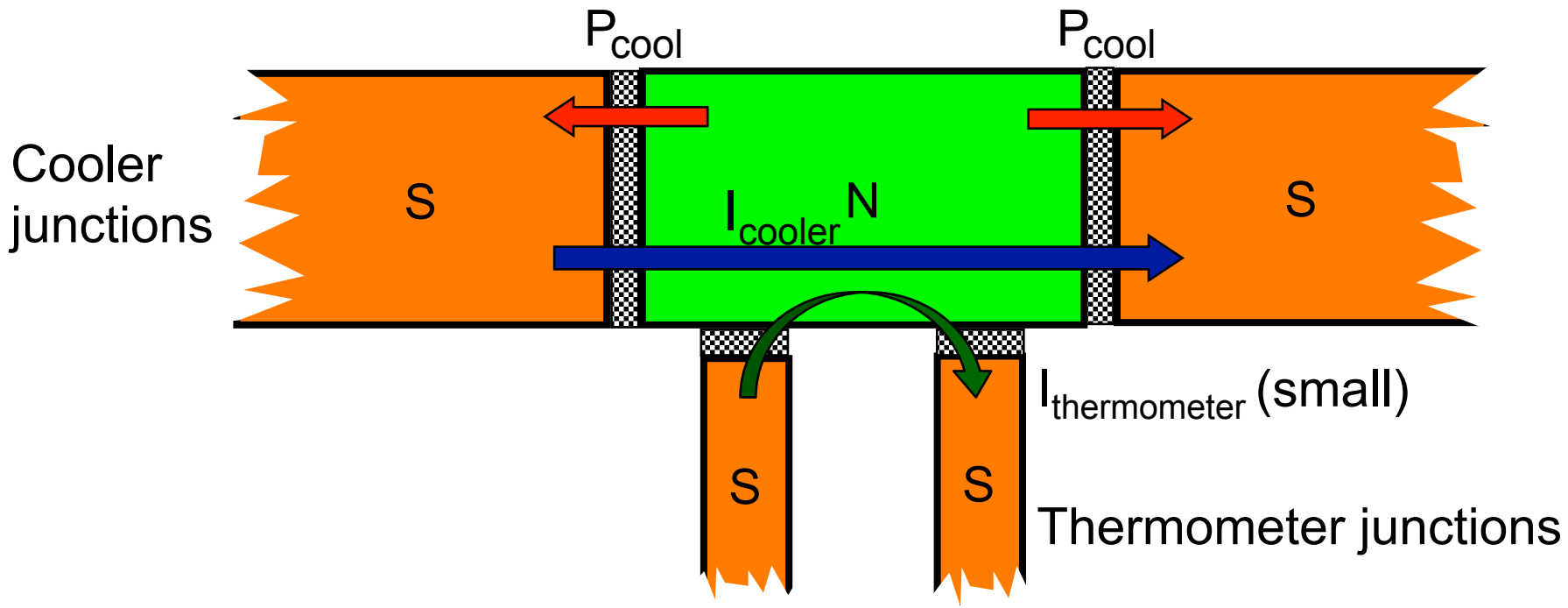

Plus two thermometer junctions for independent probing.

Electronic cooling and thermometry

Cooling from 300 mK down to 100 mK can be achieved in a S-I-N-I-S geometry.

Above the gap: qp injection and heating

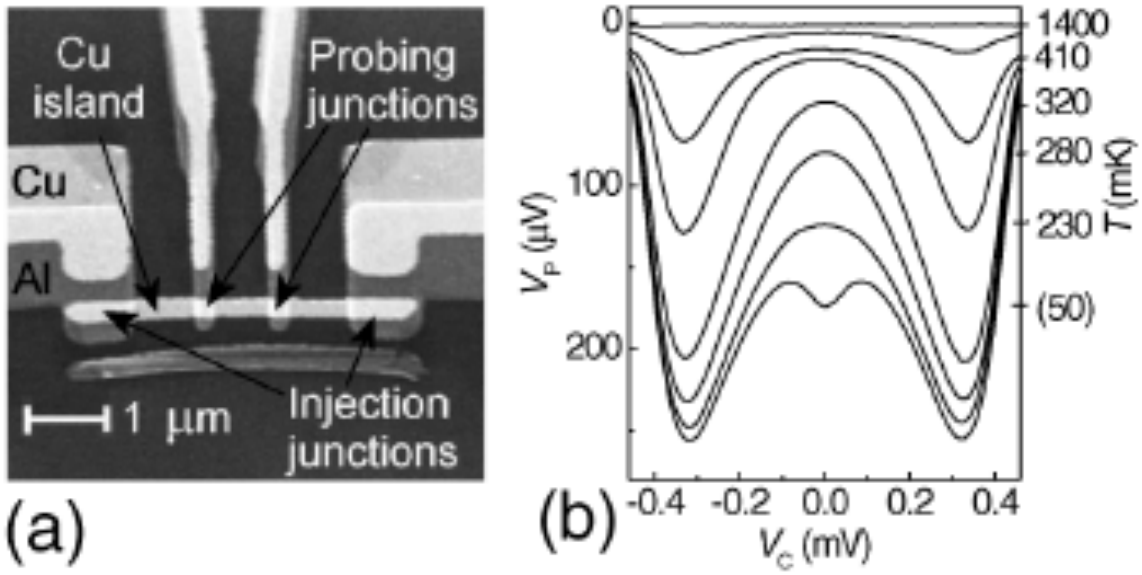

FIG. 1. Scanning electron micrograph of a typical cooler sample in (a), and cooling data in (b), where voltage V_P across the probe junctions in a constant current bias (28 pA) is shown against voltage V_C across the two injection junctions. Cryostat temperature, corresponding to the electron temperature on the N island at $V_C = 0$ is indicated on the right vertical axis. Below 100 mK this correspondence is uncertain, because of the lack of calibration and several competing effects to be discussed in the text.

J. Pekola, T.T. Heikkila, A. M. Savin, J.T. Flyktman, F. Giazotto, F.W.J. Hekking, Phys. Rev. Lett. 92, 056804 (2004): Helsinki.

Limitations of electronic refrigeration

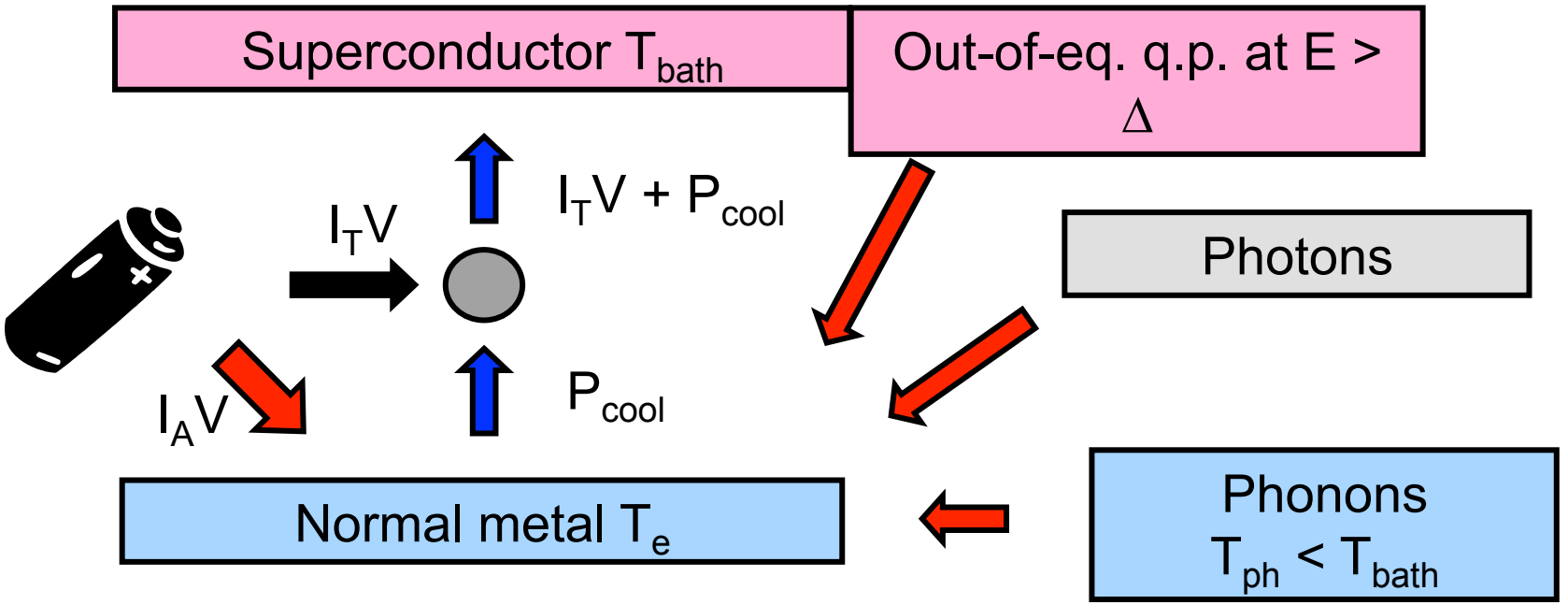

Our objective:

Understand the mechanisms coupling the cooled e- to the thermal baths.

F. Giazotto, T. T. Heikkila, A. Luukanen, A. M. Savin and J. P. Pekola, Rev. Mod. Phys. 78, 217 (2006): Helsinki.

Phonon cooling vs electron cooling

The S-I-N-I-S samples

Probe: metal strongly thermalized, no cooling.

Cooler: weakly coupled to pads, strong cooling, R_t about 1 kΩ.

No electron thermometer.

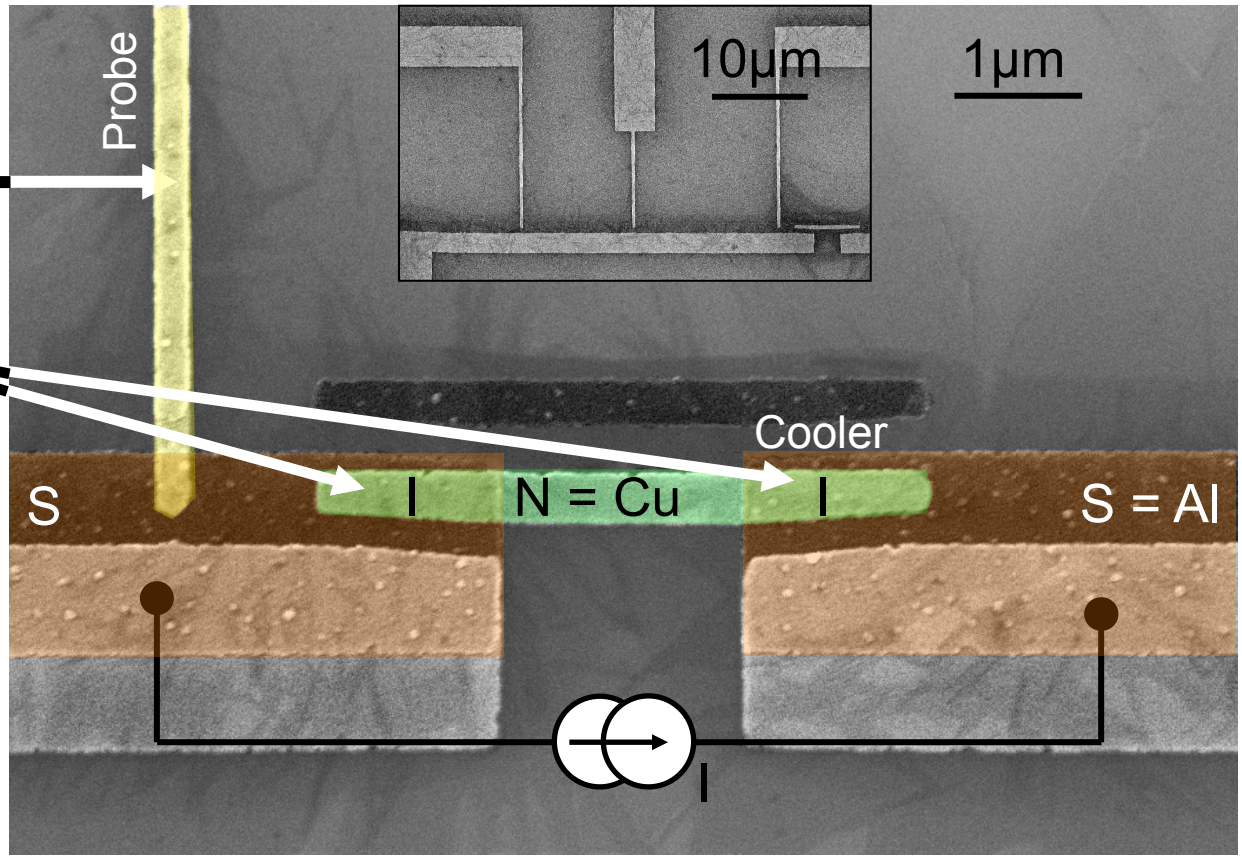

Nanofab, Institut Néel, CNRS & UJF

Al-AlO_x-Cu tunnel junctions: high stability and good reproducibility.

Al behaves as a perfect BCS superconductor.

The differential conductance

T_{base} = 320 mK

High resolution measurement (log scale)

Probe follows isothermal prediction at T_{base}.

$$eI(V) = G_T \int_{-\infty}^{+\infty} N_S(E)\left[f_S(E) - f_N(E+eV)\right]dE$$

Cooler behaves differently

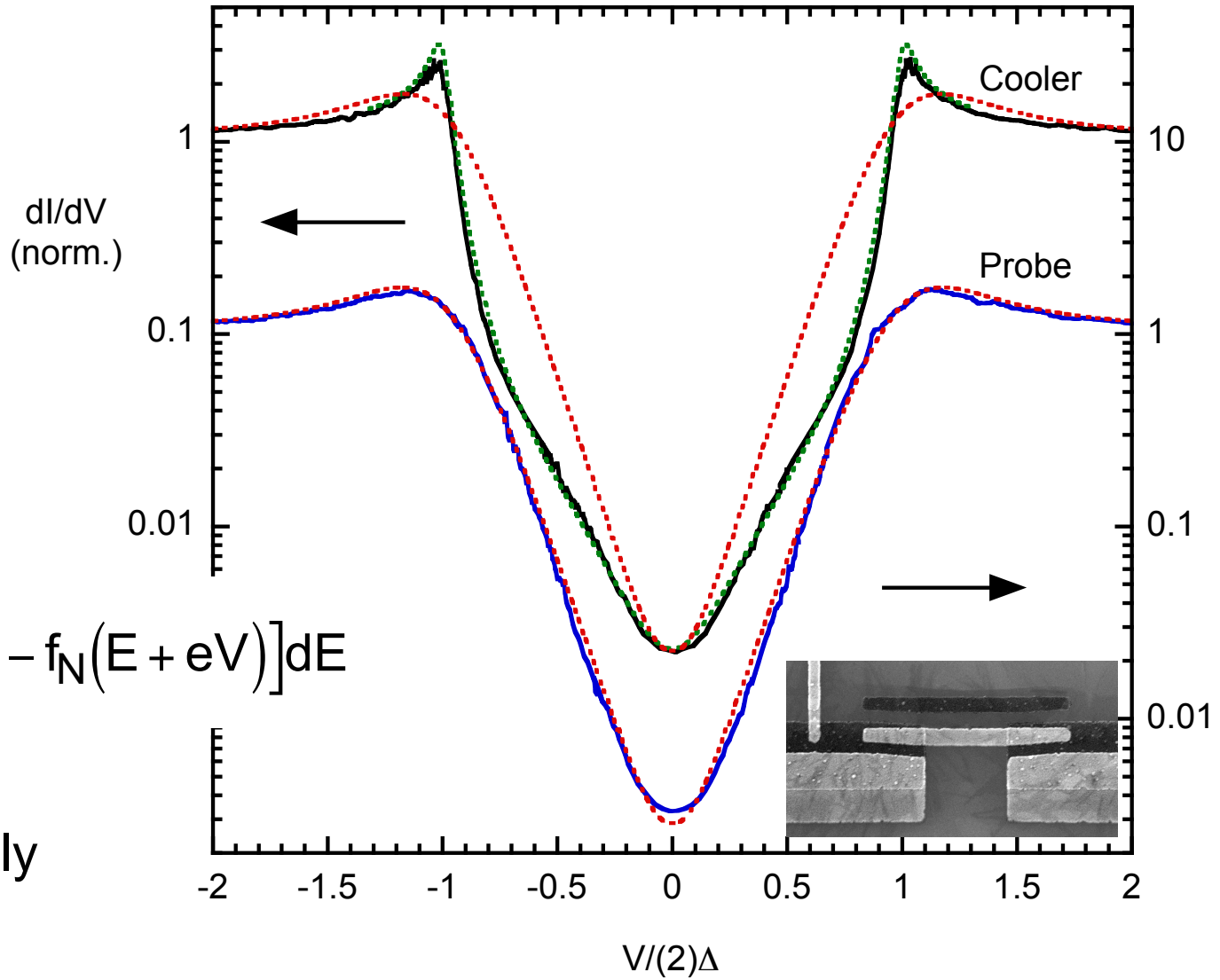

Extraction of the electron temperature

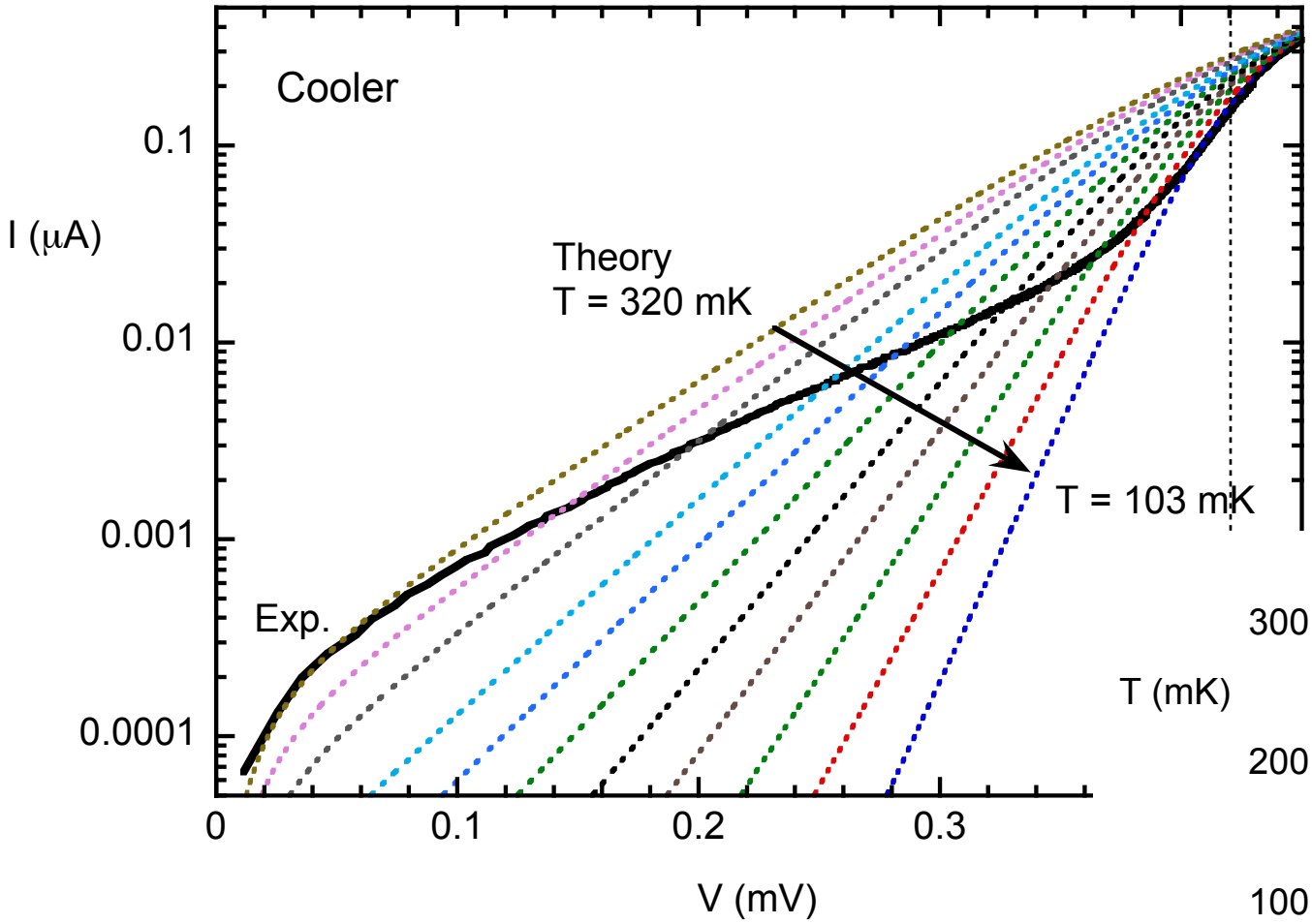

Inelastic scattering strong enough to define an electron temperature.

Superposition of exp. data with theoretical I-V

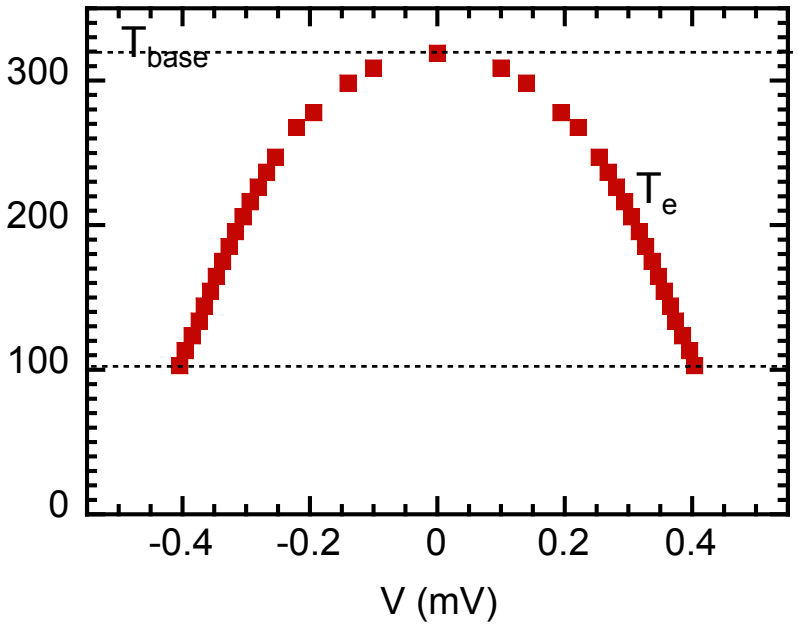

Determination of the bias-dependent electron temperature

The thermal model

Power flow from N electrons to the S electrodes remaining at bath temperature

$$P_{cool}(V) = \frac{1}{eR_N}\int_{-\infty}^{+\infty}(E - eV)N_S(E)\left[f_S(E) - f_N(E + eV)\right]dE$$

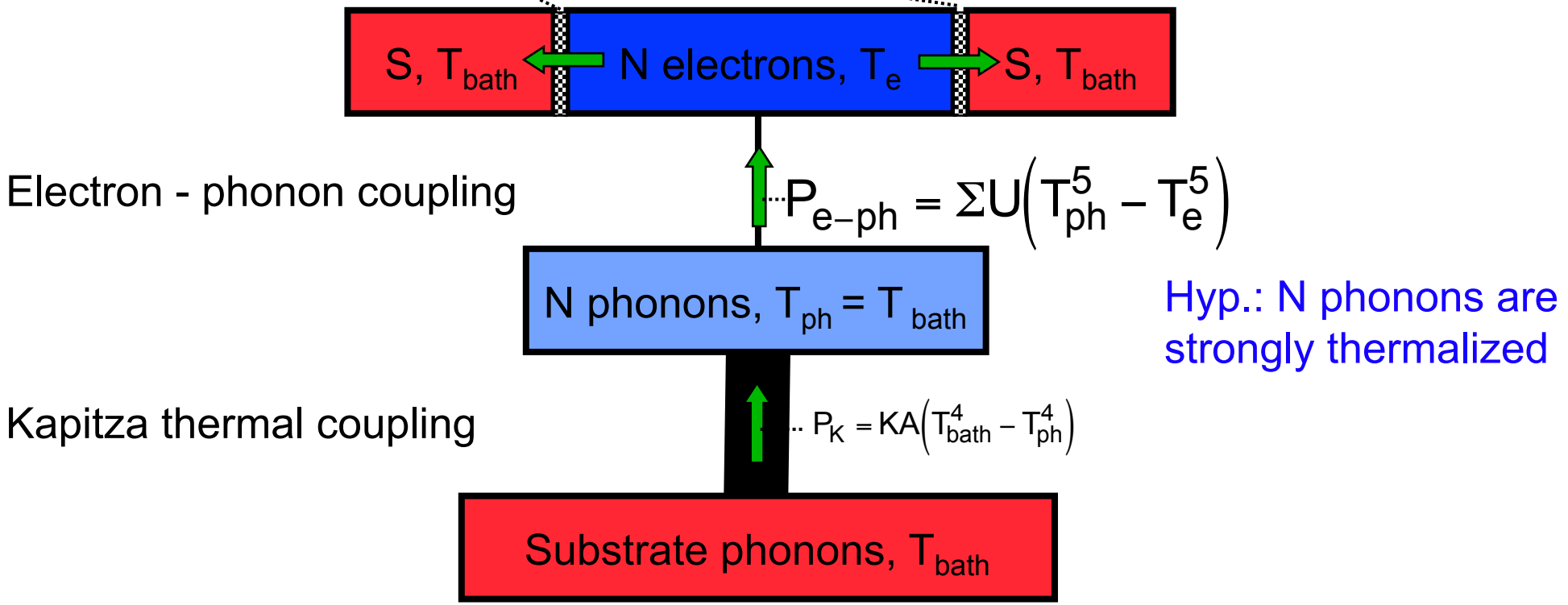

Hypothesis of phonon thermalized to the bath

Here $T_{ph} = T_{base}$

$$P_{cool} = \Sigma U\left(T_e^5 - T_{bath}^5\right)$$

$$\left(\frac{T_e}{T_{bath}}\right)^5 = 1 - \frac{1}{\Sigma U}\frac{P}{T_{bath}^5}$$

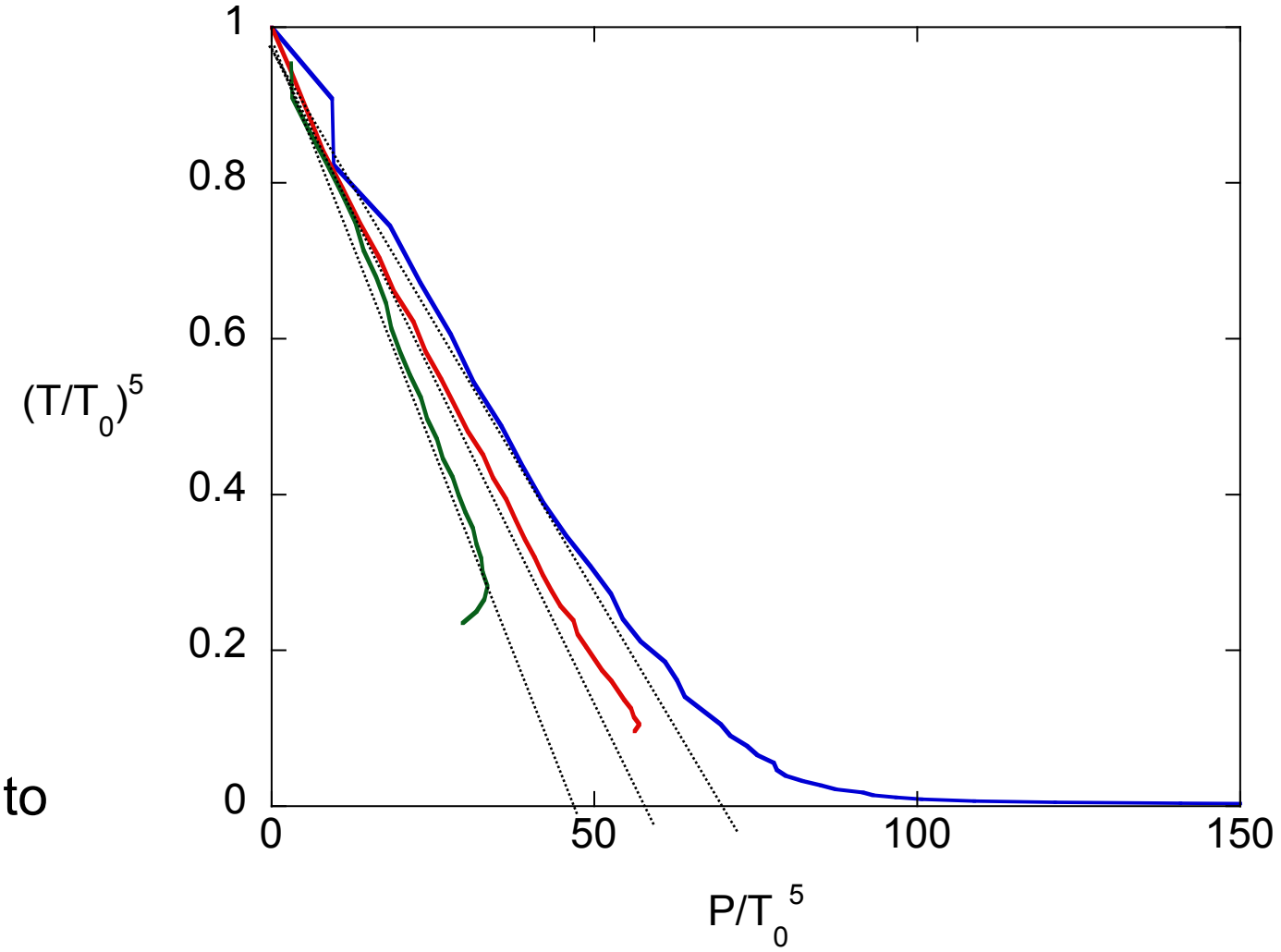

Fitted Σ varies from 0.8 to 1.2 $nW.\mu m^{-3}.K^{-5}$!

Need to consider that phonon temperature T_{ph} varies.

The thermal model

Power flow from N electrons to the S electrodes remaining at bath temperature

$$P_{cool}(V) = \frac{1}{eR_n}\int_{-\infty}^{+\infty}(E - eV)N_S(E)\left[f_S(E) - f_N(E + eV)\right]dE$$

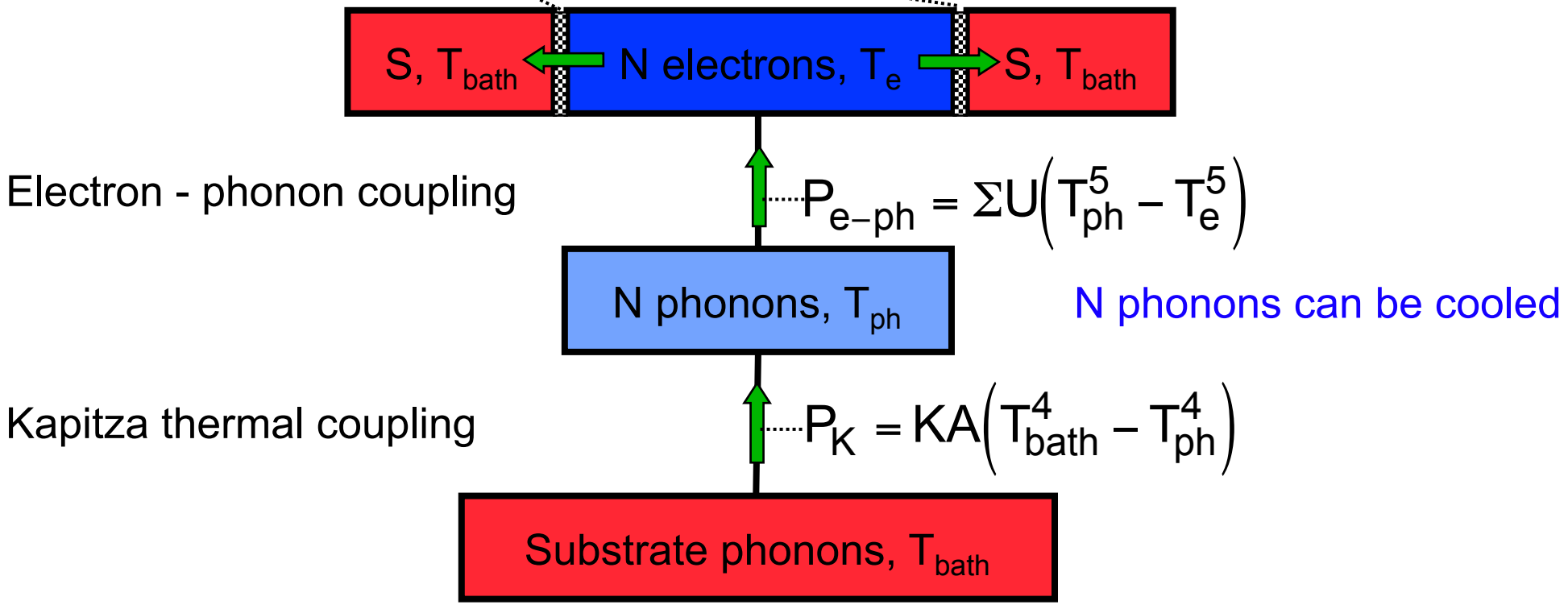

The phonon temperature

Two free fit parameters:

Σ = 2 nW.µm^{-3}.K^{-5}

KA = 66 pW.K^{-4}

Determination of both electron (T_e) and phonon (T_{ph}) temperature.

Phonons cool down by about 50 mK.

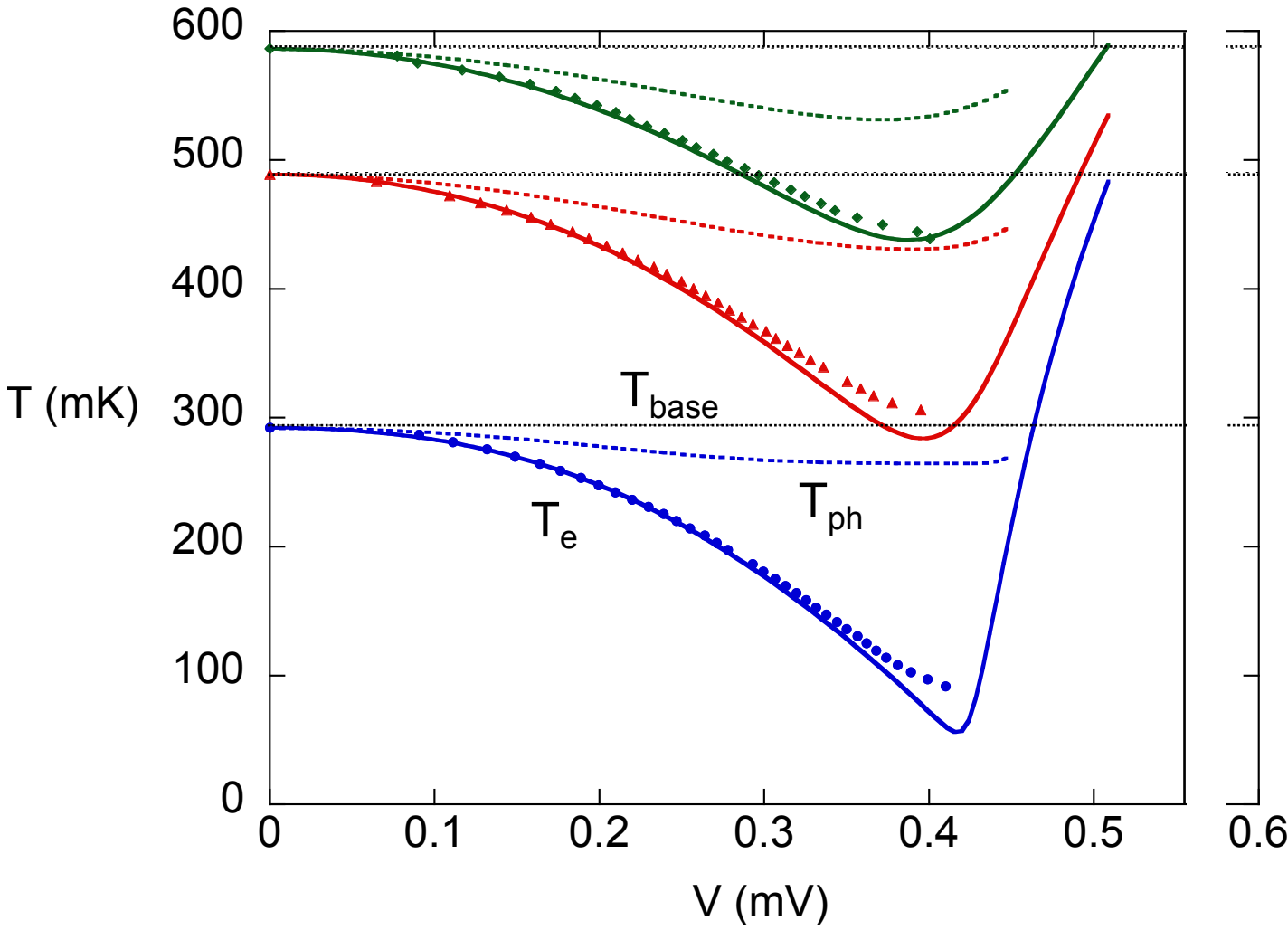

S. Rajauria, P. S. Luo, T. Fournier, F. W. J. Hekking, H. Courtois, and B. Pannetier, Phys. Rev. Lett. 99, 047004 (2007): Grenoble.

The differential conductance (again)

Consistency check:

Fit of the cooler differential conductance.

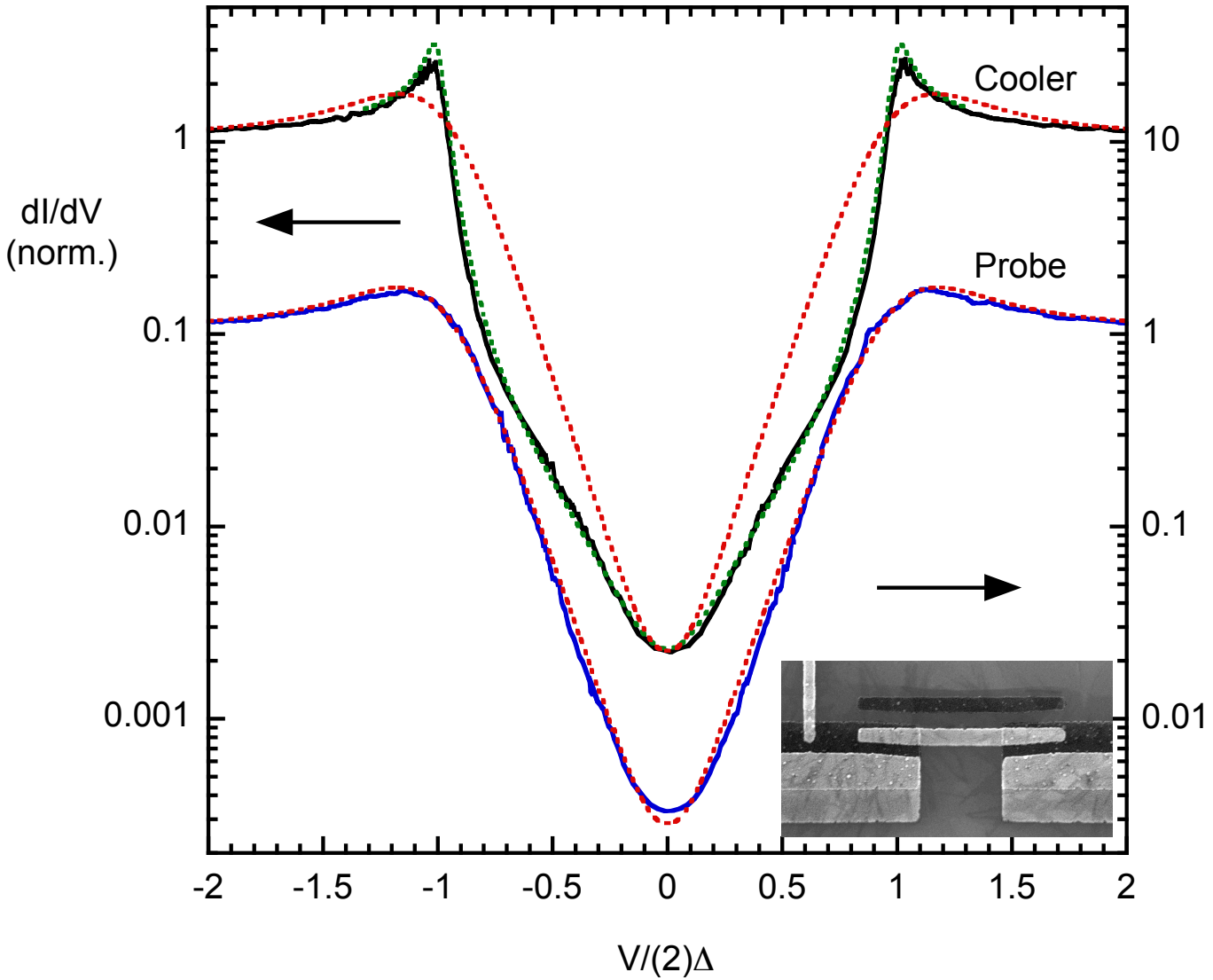

Other approaches

Quantum dot cooling (1)

Device = Drain – QD – « metal » - QD – Source

QD discrete energy spectrum open gaps, which acts as an energy filter, like the superconductor energy gap.

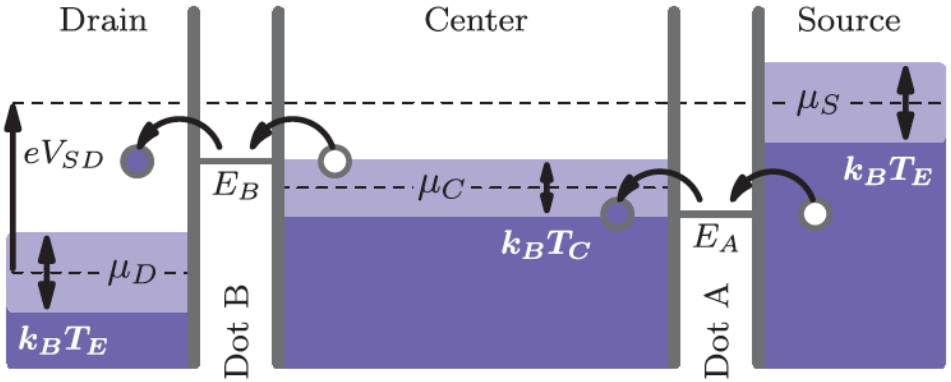

FIG. 1 (color online). QDR energies in the cooling regime. Thermal broadening in the three 2DEGs (source, center and drain) is shown by the light shading around their electrochemical potentials (μ_S, μ_C, μ_D). The net flow of an electron from source to drain removes an energy $E_B - E_A$ from the center. E_A (E_B) is the ground state addition energy of dot A (B).

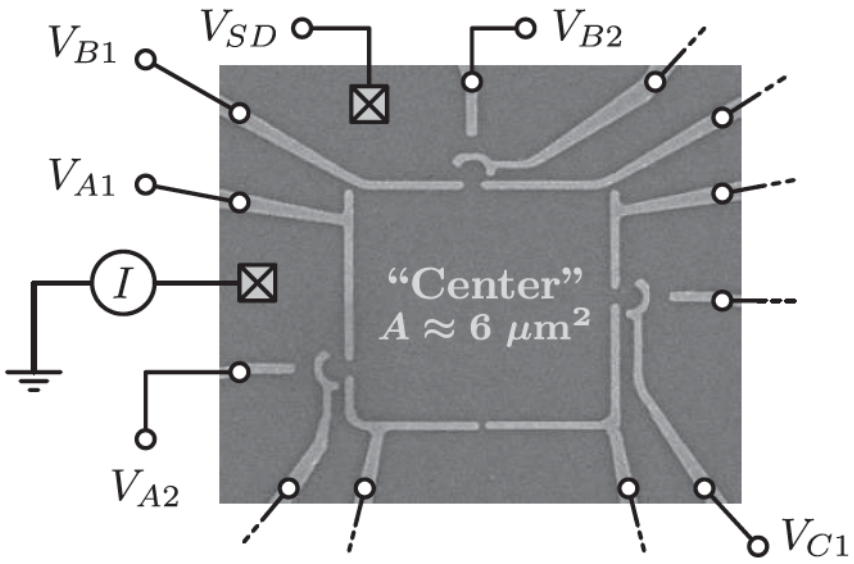

FIG. 2. SEM image of a typical device. Schematic measurement setup is also shown.

Quantum dot cooling (2)

Electronic cooling visible in the current peak assymetry.

Cooling from 280 to 190 mK.

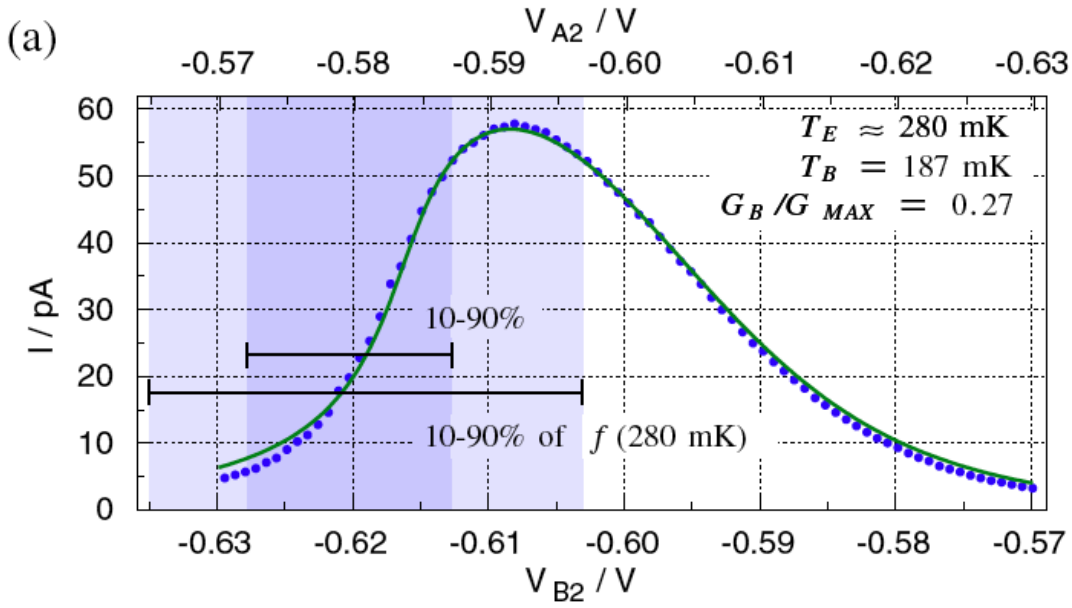

J. R. Prance, C. G. Smith, J. P. Griffiths, S. J. Chorley, D. Anderson, G. A. C. Jones, I. Farrer and D. A. Ritchie, PRL 102, 106641 (2009): Cambridge.

FIG. 5 (color online). Measurements of the QDR current while varying V_{A2} and V_{B2}. $V_{SD} = 75\ \mu$V. The mixing chamber temperature and ambient electron temperature vary between plots. In (a) and (b) the solid line is a fit to the model described in the text. The fitted G_B is given as a fraction of the peak conductance ($G_{MAX} = \max(I)/V_{SD}$). In (c) the solid line shows the best fit to the sum of two Gaussian peaks.

Applications

Applications (1)

Heat current of about 10 pW/μm^2 (= 1 W/m^2).

Need for highly-transparent and large junctions for a large cooling power: UV litho. and etching.

AlMn is a normal metal with a natural barrier similar to Al.

A.M. Clark, N. A. Miller, A. Williams, S. T. Ruggiero, G. C. Hilton, L. R. Vale, J. A. Beall, K. D. Irwin, and J. N. Ullom, Appl. Phys. Lett. 84, 625 (2005): NIST Boulder.

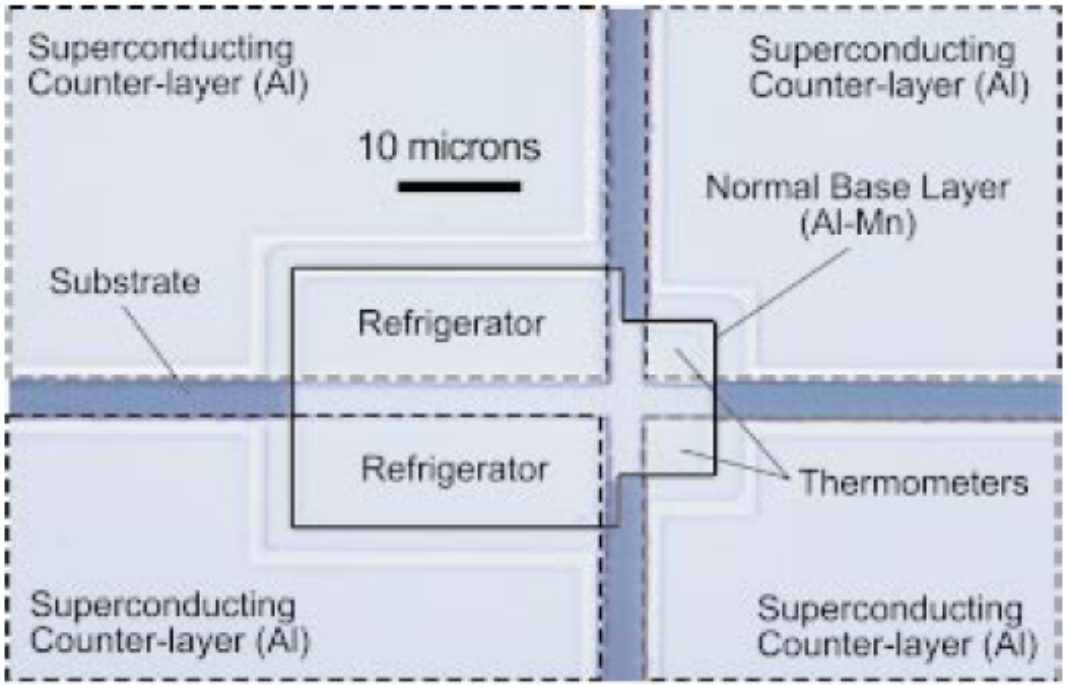

FIG. 2. (Color) Optical micrograph of device. Four superconducting counterelectrodes (outlined with dashes) contact the central normal base electrode (solid outline). An insulating layer of SiO_2 separates the base and counterelectrodes. Vias in the SiO_2 define the four NIS junctions. The device contains two refrigerator junctions, 25 μm long and 10 μm deep, and two thermometer junctions, 5 μm on each side. Additional vias in the SiO_2 provide access to normal quasiparticle traps located underneath the counter electrodes.

Applications (2)

Relevant for on chip cooling of detectors, quantum devices …

Membrane technology provides a thermal decoupling to the bath.

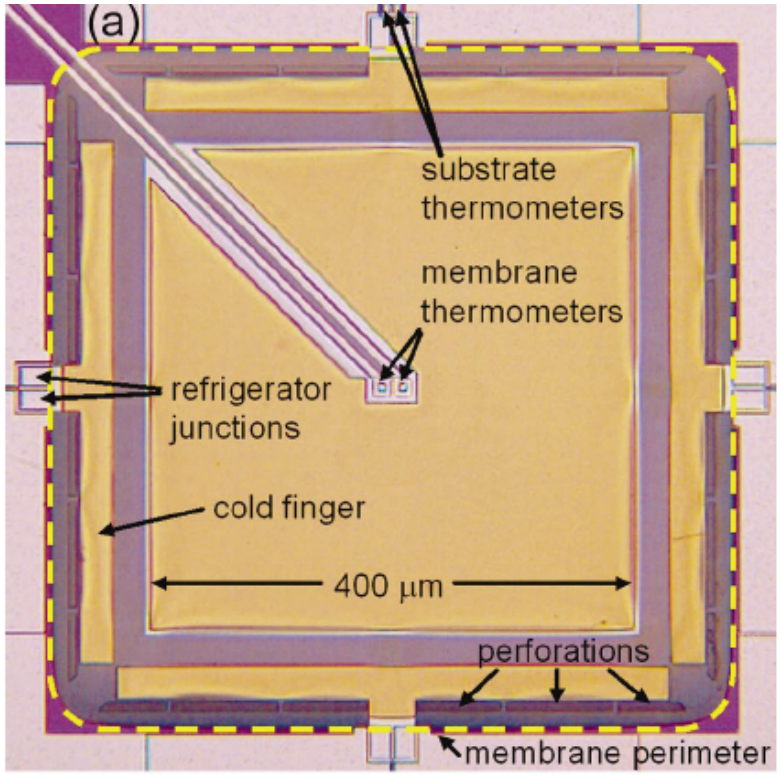

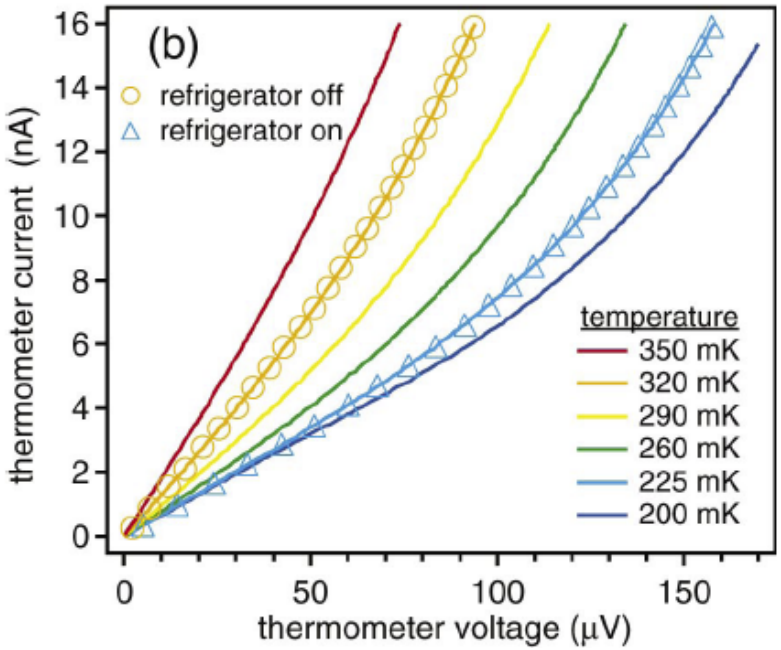

FIG. 1. (Color) (a) Optical micrograph of NIS refrigerator. Four pairs of refrigerator junctions surround a micromachined Si_3N_4 membrane. Cold fingers extend from the refrigerator junctions onto the membrane. Pairs of thermometer junctions are located at the center of the membrane and on the substrate. A 200 nm layer of Au (orange) covers the Al–Mn of the cold fingers and the center of the membrane for better thermal conductivity. There is no electrical connection between the cold fingers and the circuitry in the center of the membrane. (b) Lines show measured current–voltage curves of the membrane thermometer junctions at ADR temperatures from 350 to 200 mK. Markers show measured current–voltage curves of the membrane thermometer junctions at an ADR temperature of 320 mK with the refrigerator junctions unbiased (turned off) and biased (turned on). It can be seen that the refrigerator cools the membrane from 320 to 225 mK.

Applications (3)

A NTD bolometer is cooled from 320 mK down to 225 mK.

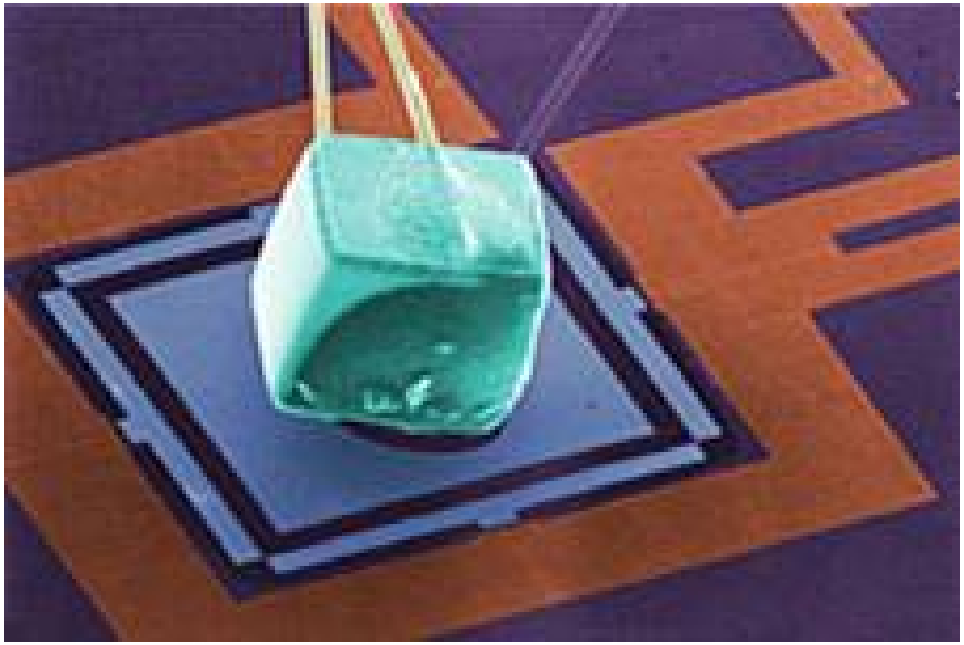

FIG. 2. Scanning electron microscope image of NIS refrigerator with attached neutron transmutation doped (NTD) germanium resistance thermometer. One of the four pairs of refrigerator junctions is circled. Additional junctions for thermometry are located beneath the NTD. The ratio of the volumes of the NTD and the refrigerating junctions is comparable to the ratio of the volumes of the Statue of Liberty and an ordinary person (about 11 000).

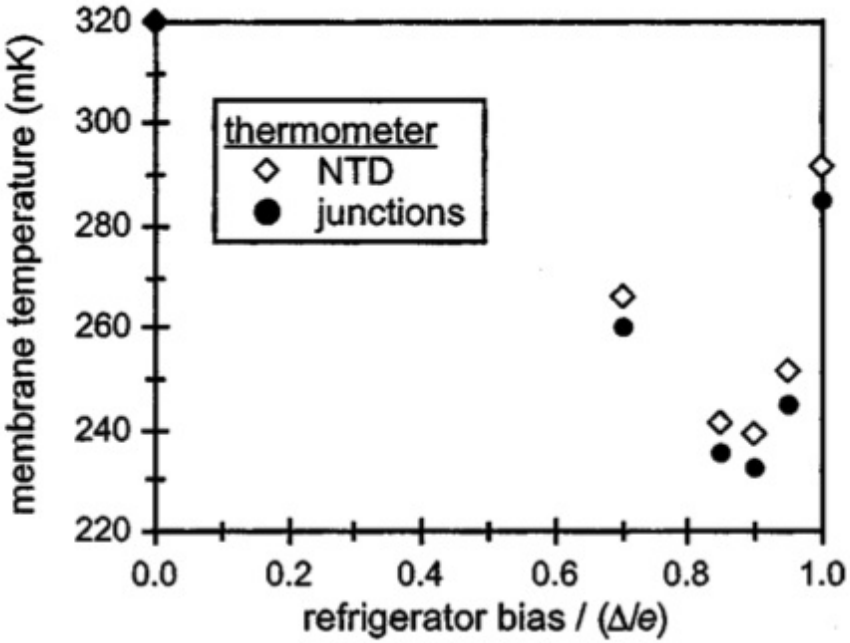

FIG. 3. Measured membrane temperature plotted vs refrigerator bias. Temperature measurements are shown for the NTD thermometer and a junction pair underneath the NTD. The peak cooling of the NTD corresponds to a tripling of its physical resistance. The peak cooling occurs for refrigerator bias values near $0.9\Delta/e$, as expected.

Cooling efficiency

Dissipated power (by the bias source) in the superconductor : $I.V$

Cooling power in the normal metal : $P_{cool} \approx I(\Delta - eV)$

At the optimum bias, thermal qp overcome the gap : $\Delta - eV \approx k_B T_e$

Efficiency $\eta = \frac{P_{cool}}{I.V} \approx \frac{\Delta - eV}{\Delta} \approx \frac{T_e}{\Delta}$

$\Delta = 1.76\ k_B\ T_c$; $T_c = 1.3$ K; $T_e = 0.1$ K $\Rightarrow$ $\eta = 4$ %

Rather low efficiency at low temperature,
Energy dissipation in the superconductor is a major issue.

Conclusion

- Why cooling several kilograms while a nanogram (the detector) is enough ?
- Electron and phonon cooling in N-I-S nano-junctions : out of equilibrium effects.
- Applications based on membrane technology, or use the cooled eletrons population as the sensor.

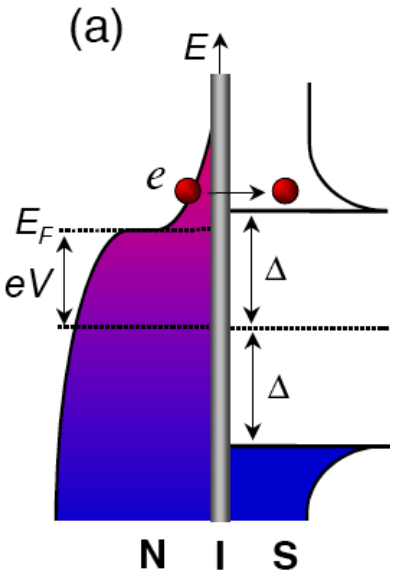

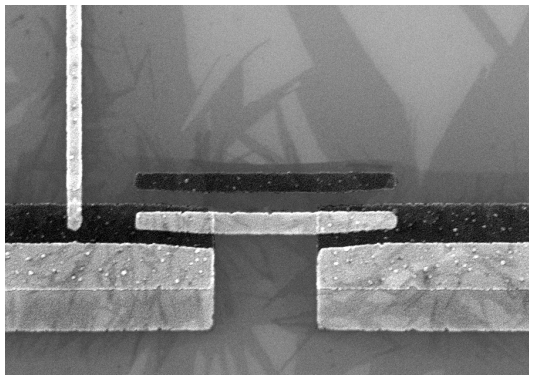

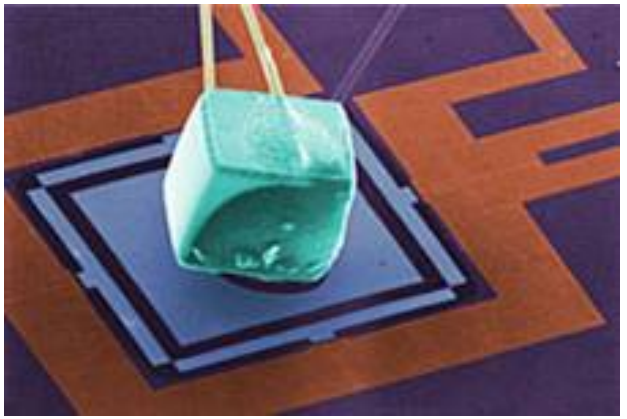

Thanks to:
MICROKELVIN
ITN Q-NET